NTNU – Trondheim
Norwegian University of
Science and Technology

Static Analysis of Fire Water Pump Module

Knut Vilhelm Størkson

Master of Science in Product Design and Manufacturing
Submission date: June 2012
Supervisor: Kjell H. Holthe, KT

Norwegian University of Science and Technology
Department of Structural Engineering

Preface

This master thesis is a collaboration between Knut Vilhelm Størkson and Frank Mohn Flatøy AS (FRAMO). The thesis originates in a project paper during the fall of 2011, where the goal was to get an overview of the theory and concepts that would be necessary for an in-depth study of one of FRAMO's products; The Fire Water Pump Module.

Througout the writing process I have worked with different computer software;

- ANSYS V14.0 (Workbench, DesignModeller and Mechanical), Analysis Software
- SpaceClaim, 3D-modelling software
- Texmaker, LaTeX-compiler
- Matlab
- Microsoft Excel

I have attended two courses over a total of 5 days in ANSYS. But other than that, all my experience is obtained through workshops and self-exploration.

All models and illustrations are self made, if it doesn't say otherwise in the "List of Figures".

I want to thank:

Kjell Holthe, my supervisor at NTNU, and Sigve Gjerstad, my supervisor at Frank Mohn Flatøy, for remarkable help and advice.

Some of my future collegeues at Frank Mohn; Tomas Laugsand Erlien, Jostein Smaamo and Ørjan Hansen.

The people from EDR, who provided courses and software free of charge, and also for the tremendeous help through their "technical support"; Bjørn Tollefsen, Kjetil Rognlien, Oddrun Myklebust, Heidi Stokke and Kirill.

The thesis was written during the spring 2012.

Trondheim, June 11, 2012

Knut Vilhelm Størkson

Knut Vilhelm Størkson

Abstract

This thesis is based on a project from the previous semester (fall 2011) and initiated by Sigve Gjerstad at Frank Mohn Flatøy AS.

The thesis introduces the FWP system and different aspects regarding a static analysis of it's main component; The FWP Module.

It takes a brief look at different meshing techniques and other choices that needs to be made in the early stages of an analysis.

A series of simple analyses are carried out to show how shell elements are the best representation for a plate structure subjected to pressure.

A series of simplified blast load analyses are presented where different choices within the Finite Element Method are compared. It's concluded that it is sufficient to consider only one of the two load steps to get the maximum values of stress and deformation. This saves us computation time with no loss of accuracy.

The analyses also conclude that a blast load analysis is dependant on a non-linear material model to get reasonable result. A linear material model assumes stress is proportional to strain, even beyond the yield strength. This results in unrealistic high stresses.

Implicit solver versus explicit solver are compared in the case of blast loading, which is a problem that requires short time increments. It is clear that the results are similar, however the computational cost is much higher for the implicit solver. It is also shown that stainless steel is more beneficial than structural steel in blast load scenarios.

Finally, model simplification is studied as yet another way to decrease the computation time. This implies simplifying solid models with a mid-surface features, representing the model with shells.

CONTENTS

LIST OF FIGURES

Fig. 2.1, 2.2, 5.1, 5.2, 6.25, 7.1 and 7.6 are pictures and models provided by Frank Mohn AS.

Fig. 4.1 is from matweb [11].

Fig. 5.3 is from Kindmann and Kraus [3].

Fig. 5.4, 5.6 and 5.7 are from the Ansys manual [8].

LIST OF TABLES

Nomenclature

Symbols:

S_d	Design load effect
R_d	Design resistance
F_d	Design load
γ_F	Partial safety factor corresponding to Design Load
F_k	Characteristic load
q	Load effect function
γ_M	Partial safety factor corresponding to Design Resistance
Y_m	Material Factor
f_y	Yield strength of the material
f_d	Design strength of the material
$barg$	Gauge pressure
ρ	Material density

Abbreviations:

COG	Centre Of Gravity
DNV	Det Norske Veritas
DOF's	Degrees Of Freedom
FRAMO	Frank Mohn AS
FWP	Fire Water Pump
HPU	Hydraulic Power Unit

1. INTRODUCTION

1.1 Background

This thesis is a follow-up on a project assignment from the previous semester, where the FWP module and it's challenges were presented. During the working process of the project, a lot of new knowledge presented itself, and this is the foundation for this thesis

1.2 Problem

The problem is stated as follows:

"The Framo Fire Water Pump is an important and demanded product in the offshore and marine industry. Since it's such a versatile product, many customers get tailor made solutions. Every time a new version of the module is designed, a strength analysis needs to be done to verify that the requirements are still satisfied. This thesis aim to find ways to improve the time between a 3D-model is presented and the analysis is completed, so that the production can start as fast as possible. The thesis will look at different load cases and constraints, and how material properties play a significant role in some cases. It will also study, and compare, different choices that can be made in the initial phase of the analysis, and the advantages and drawbacks they introduce. Some keywords are:

- Meshing techniques
- Element Types
- Explicit / Implicit
- Non-linear analysis. "

To put it short:

"Present the FWP-module and it's challenges from a static point of view, and suggest solutions ."

2. THE FWP MODULE

2.1 The Basics

The FRAMO FWP Module [1] is the main part in FRAMO's Fire Water Pump System. To get an understanding of this product it's helpful to take a brief look at the system as a whole;

The FWP System is a fire fighting system, mainly for marine and offshore installations. It comes in different sizes and with different capacities. It has a versatile design and is easily tailor made for individual installations.

The system is available both as a hydraulic system and as an electrical system. Both have their pros and cons, but the main reason for choosing the electrical system is that electricity is easier to transport over longer distances, in case the sea water lifting pump needs to be located far from the power pack. The analysis process is the same regardless of what type of system it is.

The module is basically the power pack for the FWP system, containing a booster pump, a diesel engine, a generator/HPU and other utilities required in a pump system. It is connected to a Sea Water Lift pump (Also one of FRAMO's products) which purpose is to relieve the booster pump from the work it takes to lift seawater from sea level to the deck of the vessel/installation. The module is containerized for convenience and protective purposes.

[1] Fire Water Pump Module

2.2 Requirements

When it comes to oil and gas- and also marine- installations, safety is a major priority. Delivering the fire fighting system on such installations is an enormous responsibility, and therefore there is a lot of testing and analyses that needs to be done for each individual system. There are various concerns that need to be taken into consideration to meet the high requirements regarding:

- Start-up time
- Noise
- Weight
- Dimensions
- Capacity
- Maintenance

2.3 Build Structure

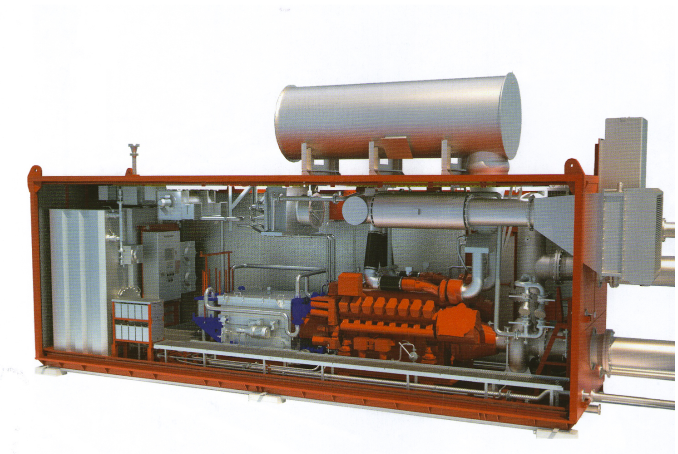

Fig. 2.1: The FWP Module

For convenience, the main components of the module is mounted on a skid inside the container. The skid is a rigid reinforced baseplate, designed for the heavy loading introduced by; the booster pump, the V16 diesel engine, the 9000 litre Fuel tank and the HPU or electric generator, depending on if it's a hydraulic or an electric system. Exhaust and ventilation are also part of the module, but they are mounted on the enclosure along with several other utilities like monitors and water mist system for fire protection.

The system is containerized because:

- The system as a whole can be tested and certified at the factory
- The installation effort is way lower then with individual components
- The container has a water mist protection system, protecting the entire system from surrounding fire, during operation
- It is easier to integrate a boxed unit into your system (especially if it is a retrofit [2]), than a number of different components with different requirements to mounting and piping and wires to connect them all.

2.4 Life Cycle

The FWP module has standard components, regardless to if it is a hydraulic or an electrical system. Some may vary, but there is always a basis to start from when tailor making a module for an installation. In most cases there are custom requirements in terms of:

Dimensions: Some installations are flexible for sizes, others have a specific length, width or height they can not exceed, it is not uncommon to have several modules on one installation, where they have to be designed differently with respect to their designated location.

Capacity: It is necessary to consider how big of an area that needs to be flooded. Most of the times this is what determines how many modules that are needed, but it can also demand a specific performance capacity from the individual module.

To sum it up, when delivering a FWP system to a big installation it is common that the process includes these steps:

- Specifications/demand
- Design
- Strength – and dynamic analysis
- Production and assembly
- Testing and certifying
- Transportation
- Installation and start-up
- Standby with periodic test runs

[2] Modification of already operational installation

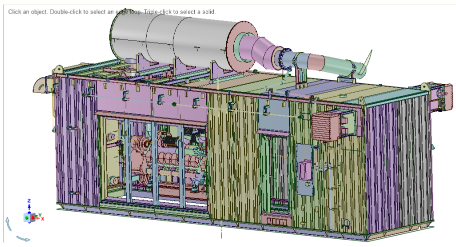

(a) Design

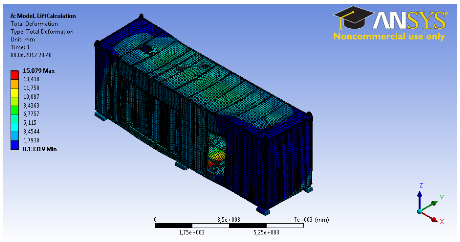

(b) Analysis

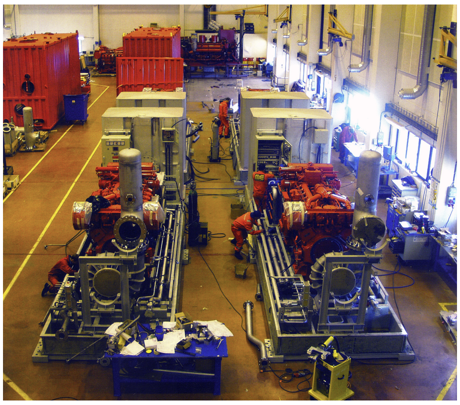

(c) Assembly

(d) Installed on platform

(e) Installed on vessel

(f) Routine test run

Fig. 2.2: The FWP Module life cycle

2.5 Challenging aspects

2.5.1 Production delay

Since this is such an important product, it is continuously being optimized. That said, the old products are still efficient, low maintenance and extremely reliable. Therefore there are no serious problems that need to be dealt with when it comes to the system itself. However, as mentioned in the previous section, there are a lot of customizations being made. And there is always room for optimization, especially when it comes to routines and efficiency.

One of the major bottle necks in the process is the transformation from the design software to the analysis software. The module is designed and tailor made through the design software, the machine- and assembly- drawings are made and the project goes from planning to production. The catch is that before production can initiate, it needs a green light from the analysis-department. The designer has created the model according to standards and true to the real product, so when the analyst gets the model, he/she needs to simplify it so that a continuous and accurate analysis can be run. Today this process can take weeks, and this can be considered as production delay (The workshop is still busy with other tasks, but the specific product is delayed). This thesis is taking a closer look at ways to improve the efficiency in the analysis process.

2.5.2 Blast loading

By looking at old reports, it's clear that one of the most significant load scenarios is from explosions. The shockwave creates a significant change in the global pressure for a short period of time, and it is not uncommon that the yield strength is exceeded in local areas. However, since this is considered an accidental scenario and because this load case is experienced over such a short period of time, local excess of stress is acceptable as long as the structural integrity is still intact.

2.5.3 Choice of material

This is not directly a challenging aspect, but balancing the requirements from the customers regarding weight, price, and strength with what areas of the product experience the greatest loading can be challenging. This is mainly the designer's task, but the thesis will take a closer look at the two most commonly used materials to get an overview of the differences they introduce.

3. FINITE ELEMENT ANALYSIS OF AN FWP MODULE

Every FWP system comes certified with an analysis-report where all the modules have been analysed according to offshore standards. There are several analyses that needs to be presented; strength and static loading, as well as dynamics. This thesis is focusing on the static part. Today there are standard procedures for how an analysis like this is done;

The unit is analysed for the following cases:

- Transport conditions, (Lifting, "Tow-out," etc)
- Operating conditions, (Accelerations from sea motion, Wind/Snow etc.)
- Accidental conditions (blast load and accidental heeling(on ships))

3.1 Assumptions

There is no need for fatigue calculations, as the structure will not be subject to significant fatigue loads. Corrosion is also considered negligible, because the module is coated.

3.2 Limit states

Limit states are scenarios with combinations of loading that are related to failure of a structure. This is a common design method used in the offshore and marine industry, and is a method to determine the line between desired and undesired states. This is considered a more rational procedure compared to the earlier traditional methods when it comes to design and strength assessment of offshore structures amongst others. This method is a requirement according to the offshore standard, DNV-OS-C101 [9], provided by *DNV* [1]

There are four main categories of limit states to consider;

FLS The fatigue limit state, related to the possibility of failure due to the effect of cyclic loading.

SLS The serviceability limit state, corresponding to the criteria applicable to normal operational use or durability. Excess will lead to failure in the functionality of a structure.

ULS The ultimate limit state, corresponding to the ultimate resistance for carrying loads. Excess will lead to failure of structure.

ALS The accidental limit state, corresponding to damage to components due to an accidental event or operation failure.

In each category a series of load combinations with safety limits are combined with respect to the consequence and recovery possibilities for each load case. They are presented in section 3.5.1.

The state of a structural element is considered to be satisfactory if the *design load effect* does not exceed the *design resistance* (Presented in section 3.3).

A limit state is defined by the equation:

$$S_d = R_d \tag{3.1}$$

Where S_d is the *Design Load Effect* and R_d the *Design Resistance*.

[1] Det Norske Veritas

3.3 Design load and resistance

Design loads and design resistances are a part of a standardized safety concept where the loading is increased and the resistance decreased, during anlyses. The concept utilizes what is called *partial safety factors* to determine the amount of adjustment. γ_F corresponds to the design load and γ_M to the design resistance. These factors are provided for each individual limit state by the DNV-OS-C101 standard [9].

The *Design load*, F_d, is obtained by multiplying the characteristic load,F_k, with the corresponding partial safety factor, γ_f:

$$F_d = \gamma_f \cdot F_k \tag{3.2}$$

If it is a variable loading, the maximum value is to be considered.

The *Design load effect*, S_d, is the least favourable combined load effect derived from the design loads:

$$S_d = q(F_{d1}...F_{dn}) \tag{3.3}$$

Where q is a load effect function.

The *Design resistance*,R_d, is determined as follows:

$$R_d = \frac{R_k}{\gamma_M} \tag{3.4}$$

Where R_k is the characteristic value of the resistance (The strength of the material for instance) and γ_M is the corresponding partial safety factor.

3.4 Loads

Loading is categorized into different subgroups according to how they tend to appear. These categories are collected from the DNV-OS-C101 [9]:

Permanent loads Permanent loads, load category G in the offshore standard, are loads with a permanent magnitude, position and direction during the period considered. They are:

- Mass of structure
- Mass of permanent ballast and equipment
- External and internal hydrostatic pressure of a permanent nature

Variable functional loads Variable functional loads, load category Q in the offshore standard, are loads which may vary in magnitude, position and direction, during the period considered, which are related to operations of the installation. They can be as follows:

- Personnel
- Stored materials, equipment, gas, fluids and fluid pressure
- Crane operational loads
- Loads from fendering
- Loads associated with installation operations
- Loads associated with drilling operations
- Loads from variable ballast and equipment
- Variable cargo inventory tor storage vessels

Environmental loads Environmental loads , load category E in the offshore standard, are loads which may vary in magnitude and direction, and are related to the environment. They can be as follows:

- Hydrodynamic loads included by waves and current
- Inertia forces
- Wind
- Earthquake
- Snow and Ice

Accidental loads Accidental loads , load category A in the offshore standard, are loads related to abnormal operations or technical failure, and can be as follows:

- Dropped objects
- Collision impact
- Explosions
- Fire
- Change of intended pressure difference
- Accidental impact from vessel, helicopter or other objects
- Unintended change of ballast distribution
- Failure of ballast pipe or unintended flooding of a hull compartment
- Failure of mooring lines

3.5 Factors

3.5.1 Load Factors

The easiest way to summarize the load combinations in the different limit states, with their corresponding load factors, γ_f, is through table 3.1.

Tab. 3.1: Load Factors

Limit State	Condition	Permanent	Variable	Environmental	Accidental
ULS	Ordinary	1.3	1.3	0.7	-
	Extreme	1.0	1.0	1.3	-
FLS		1.0	1.0	1.0	-
ALS		1.0	1.0	-	1.0
SLS		1.0	1.0	1.0	-

Tab. 3.2: Material Factors

Limit States:	SLS	ULS	ALS	FLS
Material Factor; γ_M:	1.0	1.15	1.0	1.0

3.5.2 Material Factors

3.6 Acceptance Criteria

The criterion for yield in all load cases is according to the *Von Mises Criterion*:

$$\sigma_e = \frac{1}{\sqrt{2}}\sqrt{(\sigma_x - \sigma_y)^2 + (\sigma_y - \sigma_z)^2 + (\sigma_z - \sigma_x)^2 + 6(\tau_{xy}^2 + \tau_{yz}^2 + \tau_{zx}^2)} \quad (3.5)$$

The nominal stress in the structure shall satisfy:

$$\sigma_e \leqslant \frac{f_y}{\gamma_M} = f_d$$

Where the yield strength, f_y, can be found in the material specifications and the material factor, γ_M can be found in table 3.2.

3.7 Values for the different types of loading

The values to be used for heeling, wind pressure, blast load and other types of loading are found in offshore standards or specified by the customer. They vary with each installation according to: Global location, elevation above sea level and type of installation (boat, oil rig etc.) amongst others.

4. MATERIAL PROPERTIES

The most common materials utilized for the enclosure of the FWP module are *AISI 316L: stainless steel* and *EN S355: structural steel*:

Tab. 4.1: Material properties

	EN S355	AISI 316L
Density, ρ $[kg/m^3]$	7,850	8,000
E-Module, E [MPa]	206,000	200,000
Thermal coefficient, $\alpha_{th}[1/\circ C]$	11E-6	16E-6
Poisson ratio, ν	0.3	0.3
Yield Strength [MPa]	355-315	220
Tensile Strength [MPa]	490-630	520-670
Permissible stress [MPa]	302-268	187

EN S355 has been the most common one, but stainless steel has superior properties when it comes to explosion loading. This because of it's ability for plastic deformation. Since this type of loading usually has a short impact time (0.10 to 0.15 seconds), the plasticity property will absorb the instant loading and prevent material failure.

4.1 Construction steel; EN S355

Construction steel has always been the main material utilized in the enclosure and other structural components that doesn't require enormous strength and corrosion resistance. It is a cheap (compared to higher alloy steels), machinable and weldable steel with good yield strength and it serves most purposes. The FWP module is coated for protection against corrosion.

4.2 Stainless Steel; AISI 316L

AISI 316L is the most common on the stainless steels. It has better plastic properties as well as corrosion resistance, compared to the EN355. AISI 316L has excellent resistance against corrosion.

4.3 Plastic deformation

When analysing strength, it is common to look at the material's yield strength, and then make sure it's not exceeded. The relationship between stress and strain (deformation) is approximately linear until yielding occurs. This is where the characteristics differ from material to material. Brittle material for instance, will normally have a pretty small non-linear curve before strain goes to infinity, which implies material failure. A ductile material however, will have a more significant plastic zone, where plasticity occurs. This zone is harder to calculate, and the relation between stress and strain is obtained through lab research.

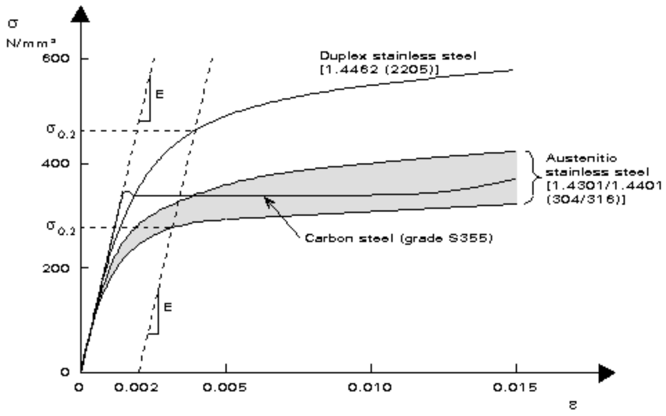

Fig. 4.1: Stress vs Strain Curve

4.4 Strain Hardening

One interesting phenomenon that may occur in the plastic zone is *Strain Hardening*, where a material is subject to loading beyond the yield strength, before it's relaxed to it's new normal state. Since the yield strength is exceeded, there will be some permanent plastic deformation, and the microstructure of the affected zone will be changed, to some degree. From a lot of research and tests, it has been proven that when the material is relaxed after plastic deformation, the strain will retract with an equivalent to elastic behaviour, even though the elastic zone is passed. From 4.1 it is clear that this leaves a permanent strain at stress equals zero, but it also results in an increased yield strength before the material will get additional plastic deformation. This phenomenon can be utilized in situations where there are concentrated stresses that exceed the yield strength in local areas.

4.5 Pros and Cons

To select the right material it is important to consider requirements such as strength, corrosion resistance and other characteristic properties. It is also worth considering practical aspects like price and how easy it is to work with. To get a quick overview of some important pros and cons for our two selected materials, they can be summed up in a table:

Tab. 4.2: HS steel vs. SS steel

	EN S355	AISI 316L
Price	Relatively Cheap	Expensive
Corrosion resistance	Poor	Excellent
Machinability	Excellent	Good
Weldability	Excellent	Good
Yield Strength	355	220
Tensile Strength	490-630	520-670
Weight	$\rho = 7850$	$\rho = 8000$

To decide which material is most beneficial, some material indices could be derived. This will not be attempted in the thesis, but could be an interesting topic for further research.

5. CHOISES IN FINITE ELEMENT METHOD

There are several significant choices that need to be considered in the preliminary phase of an analysis. Setting up everything correctly is crucial for computation time and accurate results. The first step is to import or create the model in the analysis software. In the case of FWP Modules, the models are huge and complex, and because they already have been modelled in another software it is common to use the existing model as a basis. These models have most of the features you will find on the real product, and a lot of them are insignificant for the analysis and will only complicate and slow down the computation process. These are features like:

- Rounded edges, corners and even insignificant holes
- Utilities and components that can be replaced by a simple point mass
- Complex details such as engravings etc.

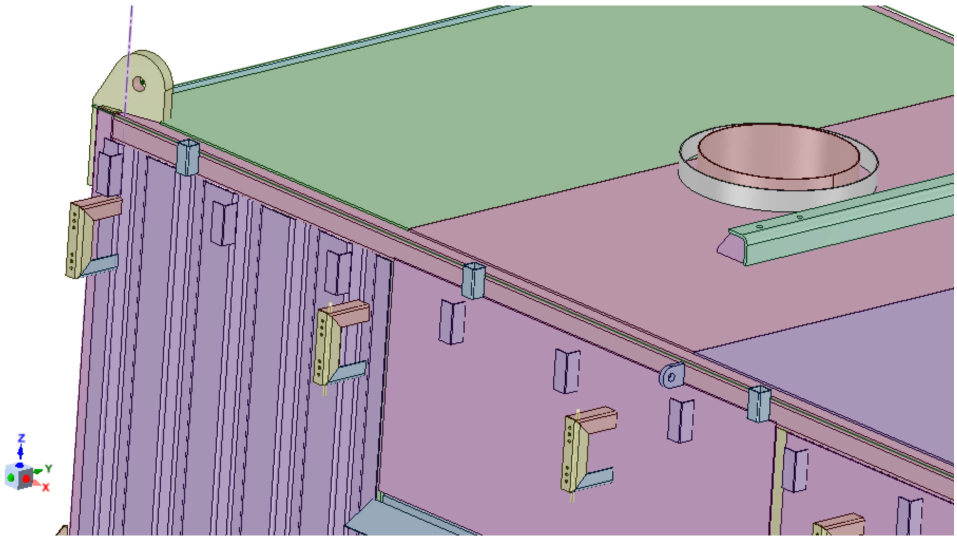

Fig. 5.1: Unnecessary details and parts

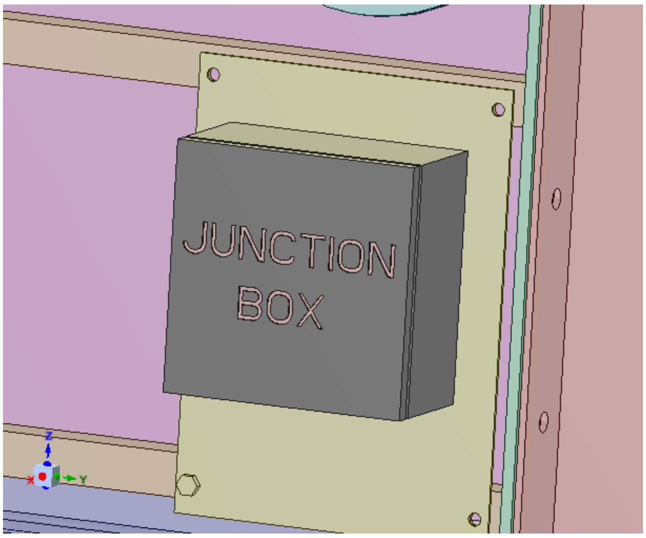

Fig. 5.2: Engraving

To put it in other words; It is highly profitable to simplify the model where it is possible. From common sense and experience the analyst should know which areas that are critical and which ones that are not. From the results it is usually possible to verify the choices by looking for concentrated stress or other problems in unexpected areas.

5.1 Element types

After simplifying the model, an important decision that needs to be made is what type of elements that should be used. This is partly related to the simplification process because the geometry is related to element choices. Examples can be simplifying a plate to be represented by surface elements with a thickness property, or representing a bolt with line elements assigned with a radius/diameter. Each case must be considered individually to make sure that the simplifications will not result in significant loss of accuracy, and also to ensure that a solution can converge and that the computation time is within reason. Element types are grouped into three main categories:

- line elements:
- surface elements:
- volume elements:

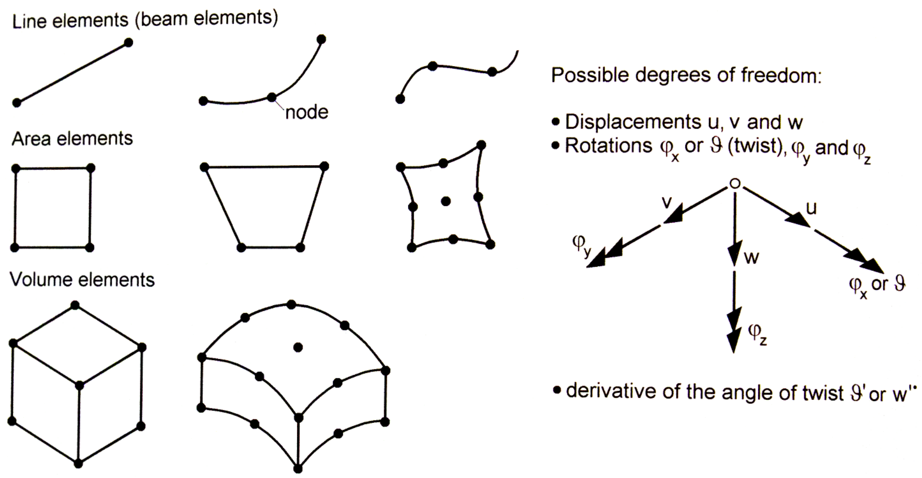

Fig. 5.3: Types of elements

5.1.1 Line elements

Line elements are one dimensional and consists of 2 nodes. If the model permits, these elements can simplify the computation process significantly. They can be assigned with a simple cross section, and are therefore valid as a representation for simple, solid, axisymmetric shapes like quadratic beams or bolts. In cases of FWP modules, the models are usually too complex for line elements to be utilized, but they could probably be used to represent the wires in the lifting part of the analysis. This is because the wires will be subject to an even and isometric tensile loading. Instead of modelling a wire and meshing it into smaller elements one line element will be sufficient for each wire. This would reduce the model's total amount of nodes (calculation points) and furthermore *Degrees of freedom*.

5.1.2 Shell elements

Shell elements are surface elements. They are commonly used for 2 dimensional problems or to describe 3D-features like plates or thin walled structures. The most common way to utilize shell elements in 3D-models, is to use the mid-planes of a structure and assign a thickness to each element according to the solid it represents. This method can save us a lot of computation time.

The number of nodes in surface elements can vary, but the ones that are used in this thesis are:

R4 The R4 shell element is the most basic shell element. It has a rectangular shape and 4 nodes, one in each vertex. It has 6 degrees of freedom (DOF's) for each node, 3 translational and 3 rotational; UX, UY, UZ, RX, RY and RZ.

R8 The R8 shell element has a similar shape to the R4 element, but in addition to nodes in each vertex it has mid-side nodes on each edge summing up to a total of 8. Each node still has 6 DOF's.

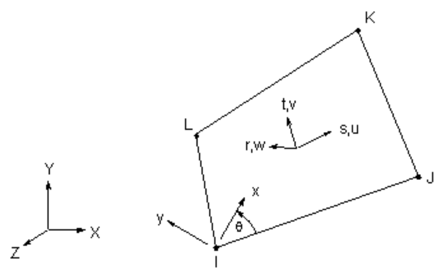

Fig. 5.4: Shell element

Shell elements are good representation for thin walled structures including plates and thin walled profiles. By converting solid structures into shell structures, a model can be simplified and still provide an accurate result. This method is called *The mid-surface technique*;

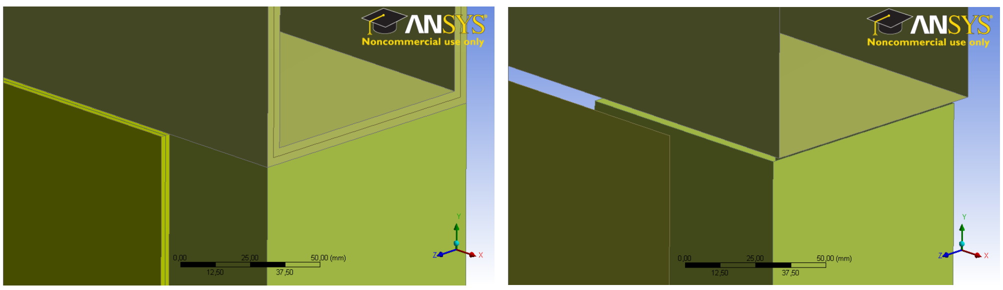

(a) Solid w/mid-surface indicated *(b)* Mid-surface

Fig. 5.5: The "mid-surface technique"

5.1.3 *Solid elements*

Solid elements are volume elements. They are a more thorough way of describing solids, and is important when uneven stress distribution is expected. In the case of this thesis it is obvious that the pad-eyes on the container will experience a lot of concentrated stress from the lifting, and it cannot possibly be distributed evenly. The optimal solid element is the perfect hexagon (dice), but most models contain arcs and advanced geometry that makes it impossible to only apply perfect hexagons, this can result in very tweaked and distorted elements which often leads to errors. Therefore the hexagons may have arced edges. In Complex geometry it is often required to make use of tetrahedron elements i addition to the hexagons.

In this thesis the following solid elements are used:

Tetrahedron This is a tetra-element with 4 or 10 nodes, depending on whether mid-side nodes are selected or not. Each node has 3 transitional degrees of freedom; UX, UY and UZ.

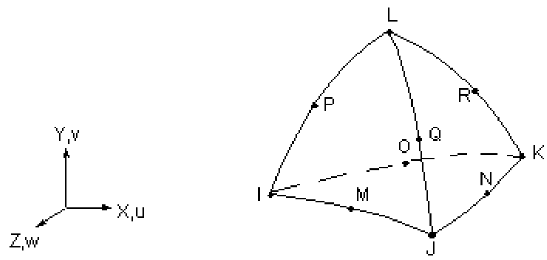

Fig. 5.6: Tetrahedron element

Hexagon This is a cubic element with 8 or 20 nodes, depending on whether mid-side nodes are chosen or not. It has three DOF's per node; UX, UY and UZ.

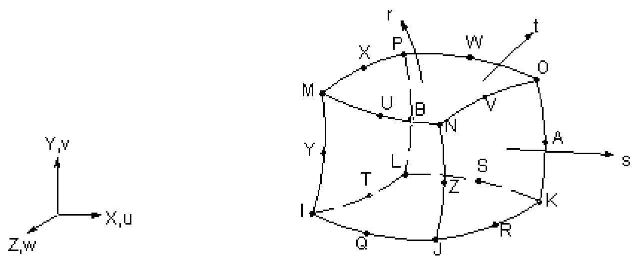

Fig. 5.7: Hexagon element

The most natural choice in the case of most FWP modules, is solid elements for the critical areas; lift ears, and shell elements for the more uniform areas to reduce computation time but preserve an accurate result.

5.2 Meshing Techniques

Meshing is the process of dividing a part/model into elements. On a complex part it can be proven wisely to have a high density of elements on critical points and bigger elements (less dense) on uniform areas. This will reduce computation time without any significant loss of accuracy.

There are several methods that can be applied to individual parts of the model, some of the most common ones are:

- Sizing: Every vertex, edge, surface or body can be applied a sizing specification.
- Sweep method: If a body is sweapable, meaning it has a constant section that can be swept, either straight or rotational, to construct the body, can be applied this specification. A surface mesh will be generated on the section and swept through the body.
- Hex-dominant method: Assigning this specification to a body will result in a mesh dominated by hexagonal elements, as far as all other specifications are met.

5.3 Element quality

After generating a mesh in *ANSYS*, it is possible to review statistics for the mesh. Here the amount of elements and nodes are presented, and also a series of different values for determining the elements quality. A graph will be displayed, and the range is editable to get a desired a span, where number of elements is displayed over the span of the quality. The elements in each group can be displayed by clicking on the corresponding bar:

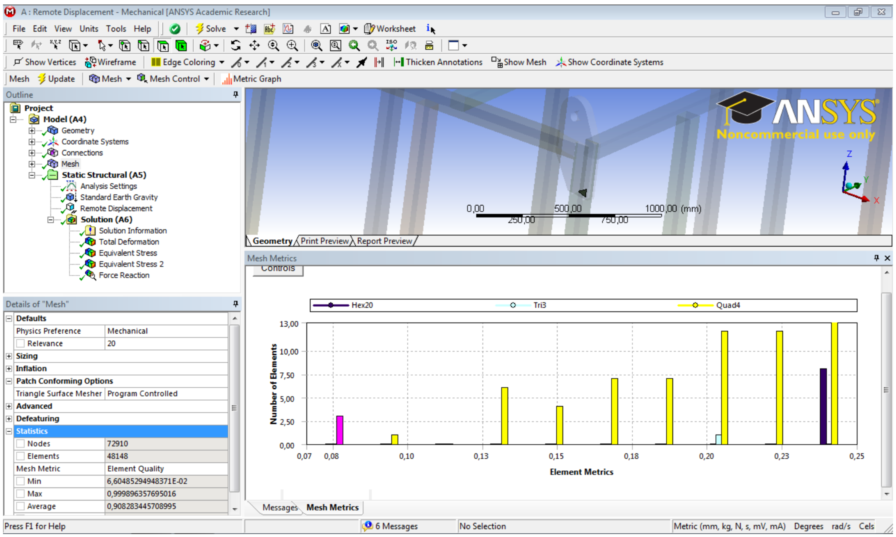

Fig. 5.8: Meshing Statistics

The *"Element Quality"* in ANSYS, is the relationship between the volume of an element an the length of it's edges. The ratio goes from 0 to 1, where 0 indicates zero volume and 1 indicates a perfect cube. It can also display factors like:

- Orthogonality
- Jacobian Ratio
- Aspect Ratio
- Skewness

Knowledge about these factors is presumed.

5.4 *Implicit/Explicit*

Another crucial choice in the Finite element method is whether to solve implicit or explicit. The basic underlying relationship between external and internal forces in final element method is:

$$[k] \cdot \{u\} = [R] \tag{5.1}$$

where: $[k]$ is the stiffness matrix $\{u\}$ is the deformation $[R]$ is the reaction force

This relationship has to be maintained at all times.

5.4.1 The implicit method

This method is a numerical approach where the values of $\{u\}$ are "guessed", the resulting force is calculated and compared with the corresponding internal energy to see if there is balance. This usually requires several attempts, and it continues until the the difference is within the *acceptance criteria*. Each calculation is called an iteration, and when a result has converged within the criteria, a load-step is completed, or a sub-step if the load-step turns out to diverge. This method is ideal for problems where the time period considered is long and for plasticity problems

5.4.2 The explicit method

The explicit method is a more direct way of solving the system. This require shorter time steps, but it doesn't require iterations like the implicit method. Hence explicit is a good choice for linear analyses or in non-linear analyses where short time steps are required, for example when blast loads are considered. It requires short time steps but each increment in computationally inexpensive compared to the implicit method.

5.5 Linear/Non-Linear

There are different reasons for a non-linear analysis to be required. One of the main reasons, is that the stiffness matrix is forced to be updated during the analysis.

- Material non-linearities: Plasticity, Creep etc.
- Geometric non-linearities: strain resistance varies with change of geometry (deformation) etc.
- Non-linear Contact boundary conditions: Contact conditions varying with displacement etc.
- Non-linear Force boundary conditions: Forces depending on deformation, like wind loads or blast loads etc.

5.5.1 Linear analysis

This is of course a preferable choice where it's sufficient. Because the system's stiffness matrix is calculated only once. To run a linear analysis the following assumptions needs to be made:

- Hook's law is valid without restrictions
- Negligible deformation influence on system
- Structural and geometric imperfections are neglected

5.5.2 Non-linear analysis

This is logically a more precise way of analysing, and it is necessary when dealing with non-linear conditions like mentioned above.

6. COMPARISONS THROUGH SIMPLE ANALYSES

To compare the different options and their significance in the previous chapter a series of simple analyses has been rendered. It is natural to take a closer look at blast loading since this is a non-linear analysis where there are room for a series of comparisons.

6.1 Preliminary analysis

To determine what type of elements that best represent the thin plates of the wall, a simple preliminary analysis that is possible to validate through exact calculations should be done. Thin plates are characterized by a thickness less than 5 % of the span in the two other directions. They do not qualify for normal beam theory so it is required to apply plate theory. There are several different methods that can be used, but to get an answer as exact as possible, a symmetric plate with a moderate pressure and fixed displacement with free rotations on each edge should be considered. In this case Navier's solution is valid, and will provide an exact result.

6.1.1 Assumptions

A square metal plate of *EN S355: construction steel* is the basis for this analysis:

The values that are used are:

Tab. 6.1: Conditions

width (a) [mm]	500
length (b) [mm]	500
Thickness (t) [mm]	4
E-modulus [MPa] ($= N/mm^2$)	206 000
Poissons' Ratio (ν)	0,3
Load (q_0) [MPa] ($= N/mm^2$)	0,015
distance from centreline to surface (z) [mm]	2

6.1.2 The model

The model is a square plate measuring 500x500x4 mm. with free support on all four edges, to satisfy Navier's equation (6.4).

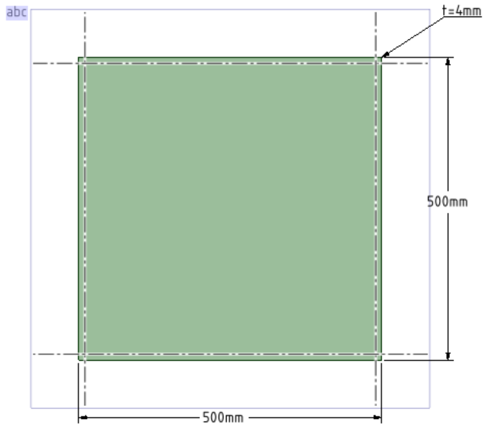

Fig. 6.1: Model for the preliminary analysis

6.1.3 The excact values

Navier's plate solution can be calculated by following these steps:

$$\begin{aligned} q_{mn} &= \tfrac{4}{a\cdot b}\int_0^a\int_0^b q(x,y)\sin\tfrac{m\pi x}{a} sin\tfrac{n\pi y}{b} dydx \\ &= \tfrac{4\cdot q_0}{a\cdot b}\int_0^a\int_0^b \sin\tfrac{m\pi x}{a} sin\tfrac{n\pi y}{b} dydx, \text{ In our case} \end{aligned} \tag{6.1}$$

$$n = \{1, ..., N\}\ ,\ m = \{1, ..., M\}$$

$$q_{mn} = \begin{cases} 0 & \text{if } n \text{ or } m \text{ are even} \\ \frac{16\cdot q_0}{a\cdot b\cdot\pi^6} & \text{if } n \text{ and } m \text{ both are odd} \end{cases} \tag{6.2}$$

$$w_{mn} = \frac{q_{mn}}{D\pi^4\left[\left(\frac{m}{a}\right)^2 + \left(\frac{n}{b}\right)^2\right]^2} \tag{6.3}$$

$$D = \frac{Et^3}{12\left(1-\nu^2\right)}$$

$$w(x,y) = \sum_{m=1}^{M}\sum_{n=1}^{N} w_{mn}\sin\frac{m\pi x}{a}\sin\frac{n\pi y}{b} \tag{6.4}$$

$$w(x,y) = \sum_{m=1}^{M}\sum_{n=1}^{N}\frac{16q_0}{(2m-1)(2n-1)D\pi^6\left(\frac{(2m-1)^2}{a^2}+\frac{(2n-1)^2}{b^2}\right)^2}\left[\sin\frac{(2m-1)\pi x}{a}\sin\frac{(2n-1)\pi y}{b}\right] \tag{6.5}$$

$$\sigma_x = -\frac{zE}{1-\nu^2}\left(\frac{\delta^2 w}{\delta x^2} + \nu\frac{\delta^2 w}{\delta y^2}\right) \tag{6.6}$$

$$\sigma_x = -\frac{zE}{1-\nu^2}\left(\frac{\delta^2 w}{\delta y^2} + \nu\frac{\delta^2 w}{\delta x^2}\right) \tag{6.7}$$

$$\tau_{xy} = -\frac{zE}{1-\nu^2}\left(1-\nu\right)\frac{\delta^2 w}{\delta x\delta y} \tag{6.8}$$

The easiest way to get the exact solution is through a computation software. Through *Matlab* with error tolerance of 1 eps [1] the results will be as follows:

[1] $1eps = 2.2204E-16$

Tab. 6.2: Excact solutions through Matlab

Max Deformation [mm]	3.15445504882141
Max σ_x [MPa]	67.3402213802704
Max σ_y [MPa]	67.3402213826199
Max $\tau_x y$ [MPa]	45.6782533024813

Note that $\sigma_x = \sigma_y$, which makes sense because of the symmetry.

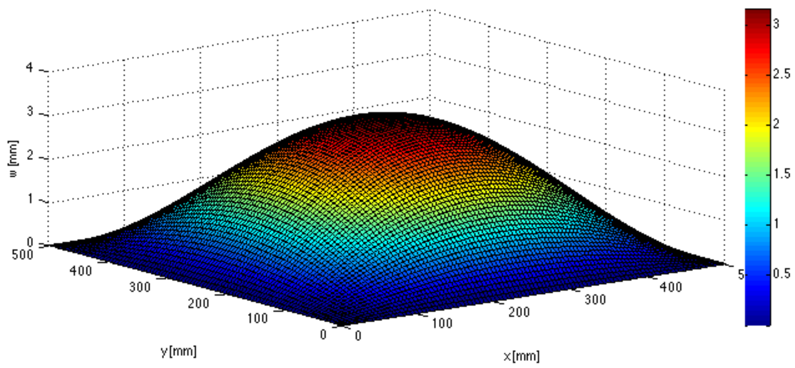

Fig. 6.2: Deformation

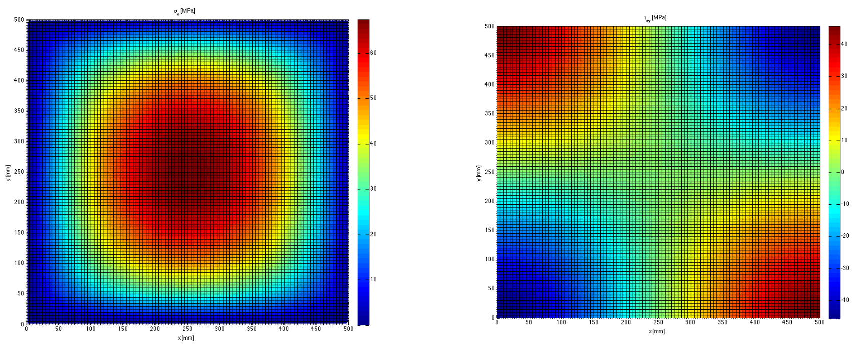

(a) Normal Stress

(b) Shear Stress

Fig. 6.3: Stresses

6.1.4 *Software analyses*

To get a good overview, four different scenarios for each setting will be studied, where the amount of DOF's [2] is varied from 100 to 100 000. To get values from the same point in all the analyses it's important with an even number of elements, so that there always is a node in the centre of the plate. This is the first priority. The second one is coming as close to 10^2, 10^3, 10^4 and 10^5 DOF's as possible.

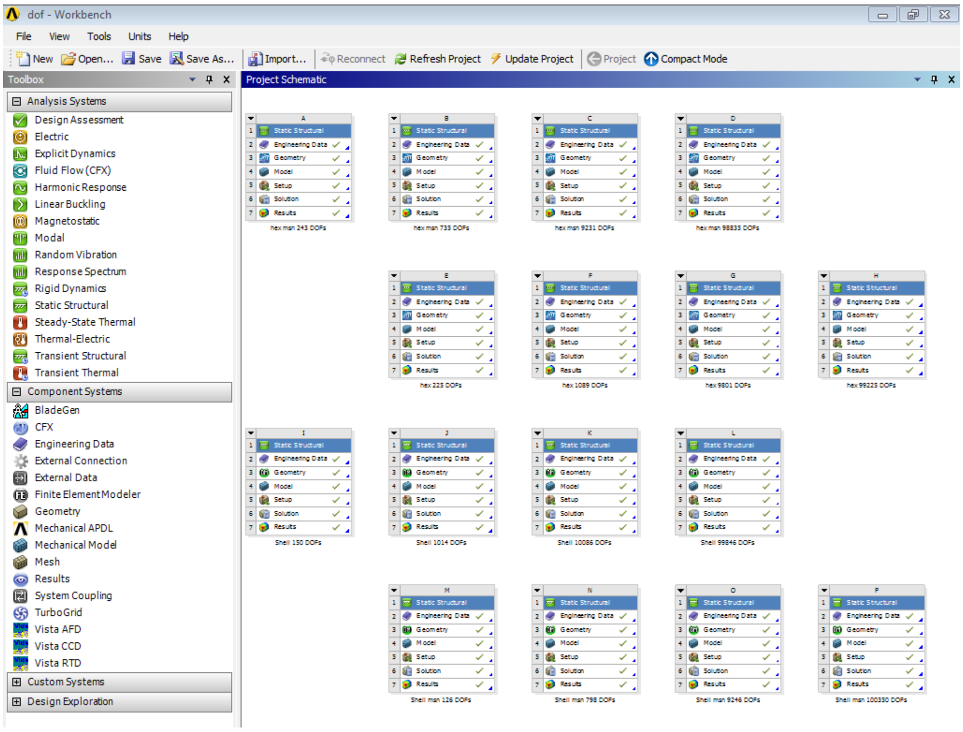

Fig. 6.4: Set-up in Ansys

[2] Degrees of freedom

hexagonal elements

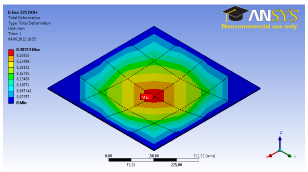

(a) Deformation

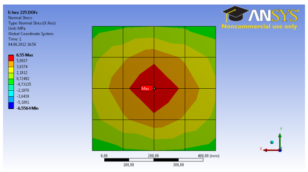

(b) Normal Stresses

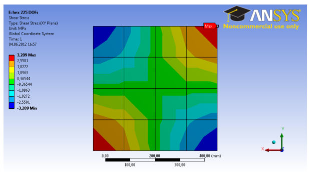

(c) Shear Stress

Fig. 6.5: Preliminary analysis with solid elements: 225 DOF's

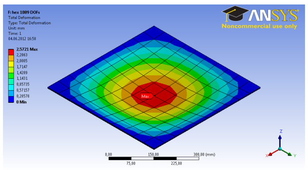

(a) Deformation

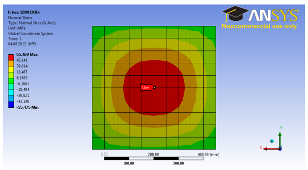

(b) Normal Stresses

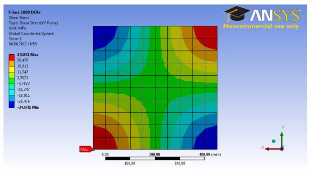

(c) Shear Stress

Fig. 6.6: Preliminary analysis with solid elements: 1089 DOF's

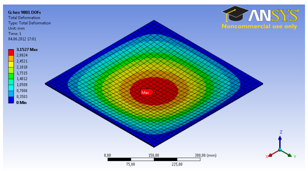

(a) Deformation

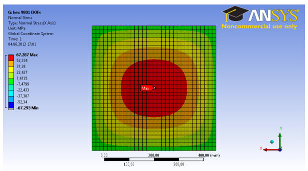

(b) Normal Stresses

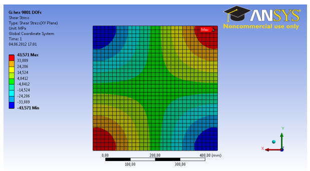

(c) Shear Stress

Fig. 6.7: Preliminary analysis with solid elements: 9801 DOF's

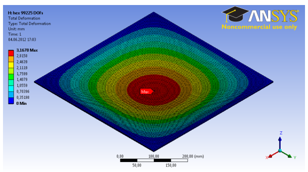

(a) Deformation

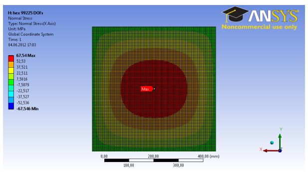

(b) Normal Stresses

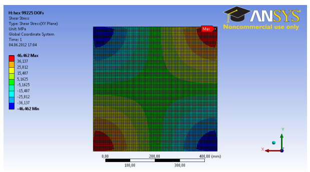

(c) Shear Stress

Fig. 6.8: Preliminary analysis with solid elements: 99225 DOF's

Solid hexagonal elements with midside nodes

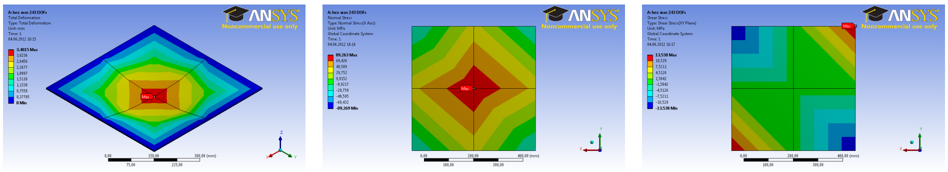

(a) Deformation (b) Normal Stresses (c) Shear Stress

Fig. 6.9: Preliminary analysis with solid elements w/ midside nodes: 243 DOF's

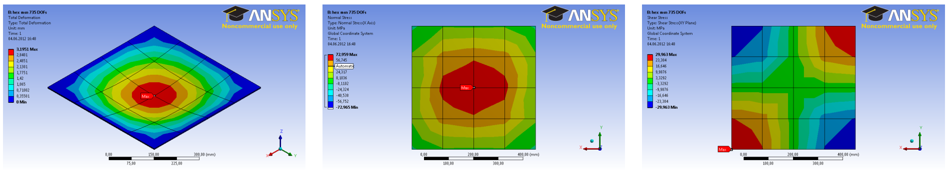

(a) Deformation (b) Normal Stresses (c) Shear Stress

Fig. 6.10: Preliminary analysis with solid elements w/ midside nodes: 735 DOF's

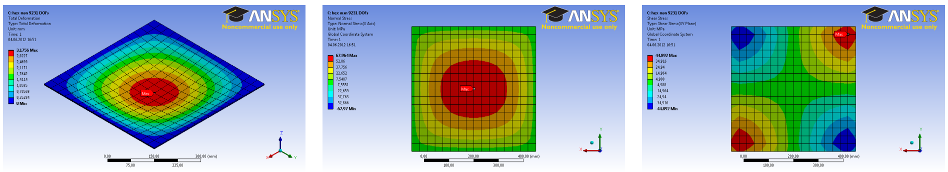

(a) Deformation (b) Normal Stresses (c) Shear Stress

Fig. 6.11: Preliminary analysis with solid elements w/ midside nodes: 9231 DOF's

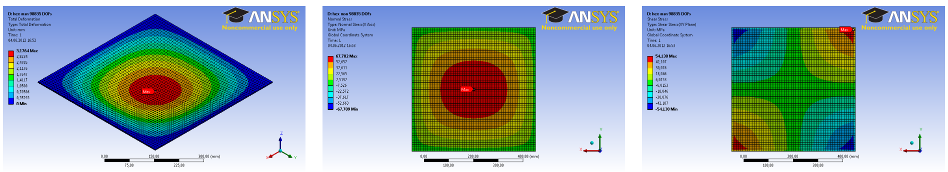

(a) Deformation (b) Normal Stresses (c) Shear Stress

Fig. 6.12: Preliminary analysis with solid elements w/ midside nodes: 98835 DOF's

Shell elements

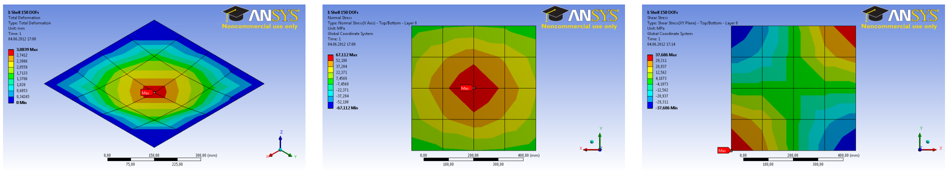

(a) Deformation (b) Normal Stresses (c) Shear Stress

Fig. 6.13: Preliminary analysis with shell elements: 150 DOF's

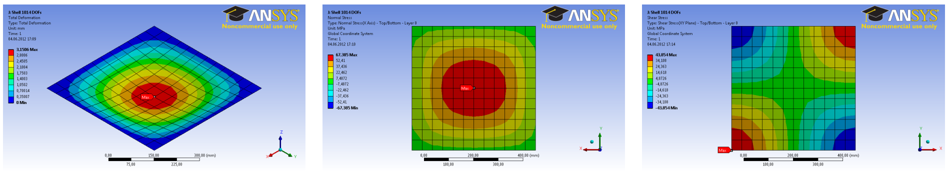

(a) Deformation (b) Normal Stresses (c) Shear Stress

Fig. 6.14: Preliminary analysis with shell elements: 1014 DOF's

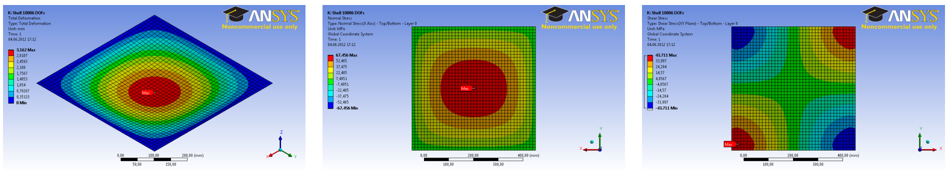

(a) Deformation (b) Normal Stresses (c) Shear Stress

Fig. 6.15: Preliminary analysis with shell elements: 10086 DOF's

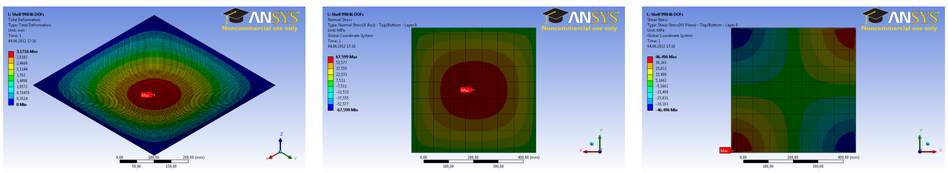

(a) Deformation (b) Normal Stresses (c) Shear Stress

Fig. 6.16: Preliminary analysis with shell elements: 99846 DOF's

Shell elements with midside nodes

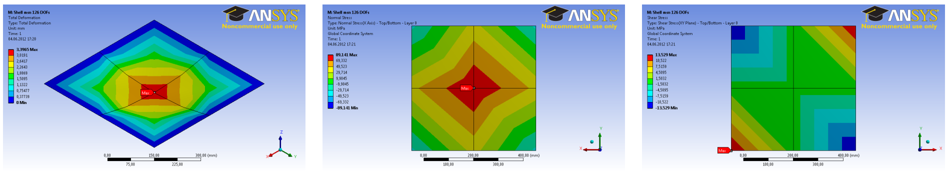

(a) Deformation (b) Normal Stresses (c) Shear Stress

Fig. 6.17: Preliminary analysis with shell elements w/ midside nodes: 126 DOF's

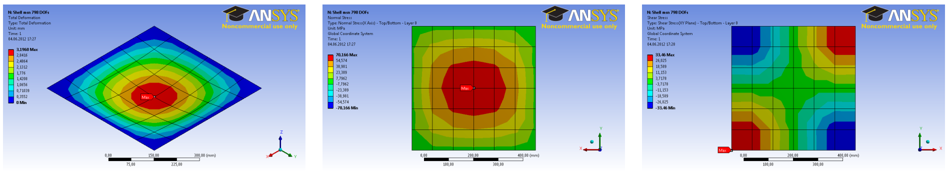

(a) Deformation (b) Normal Stresses (c) Shear Stress

Fig. 6.18: Preliminary analysis with shell elements w/ midside nodes: 798 DOF's

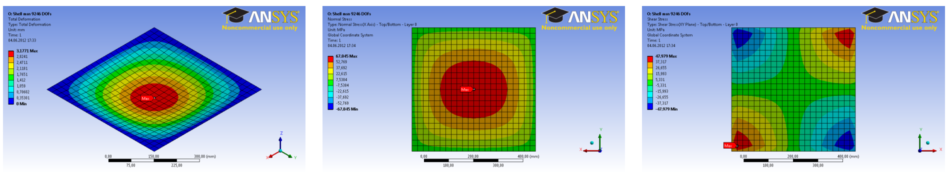

(a) Deformation (b) Normal Stresses (c) Shear Stress

Fig. 6.19: Preliminary analysis with shell elements w/ midside nodes: 9246 DOF's

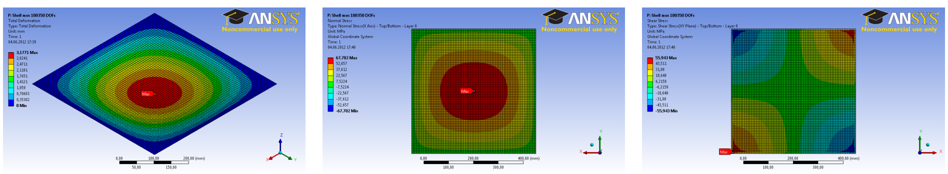

(a) Deformation (b) Normal Stresses (c) Shear Stress

Fig. 6.20: Preliminary analysis with shell elements w/ midside nodes: 100350 DOF's

6.1.5 Results and conclusion

	# of elements	# of nodes	DOFs per node	# of DOFs	Max deform	Error def	Max σ	Error σ	Max τ	Error τ
	-	-	-	-	[mm]	[mm]	[MPa]	[MPa]	[MPa]	[MPa]
Exact	-	-	-	-	3.1545	-	67.3402	-	45.6783	-
SOLID 186										
	32	75	3	225	0.30213	2.85233	6.5564	60.784	3.289	42.389
	200	363	3	1089	2.5721	0.58236	55.475	11.865	34.041	11.637
	2048	3267	3	9801	3.1527	0.00176	67.293	0.0472	43.571	2.1073
	21632	33075	3	99225	3.1678	0.01334	67.546	0.2058	46.462	0.7837
SOLID 186 w midside nodes										
	8	81	3	243	3.4015	0.24704	89.269	21.929	13.538	32.14
	32	245	3	735	3.1951	0.04064	72.965	5.6248	29.963	15.715
	512	3077	3	9231	3.1756	0.02114	67.97	0.6298	44.892	0.7863
	5832	32945	3	98835	3.1764	0.02194	67.709	0.3688	54.138	8.4597
SHELL 181										
	16	25	6	150	3.0839	0.07056	67.112	0.2282	37.686	7.9923
	144	169	6	1014	3.1506	0.00386	67.385	0.0448	43.854	1.8243
	1600	1681	6	10086	3.162	0.00754	67.456	0.1158	43.711	1.9673
	16384	16641	6	99846	3.1716	0.01714	67.599	0.2588	46.496	0.8177
SHELL 181 w midside nodes										
	4	21	6	126	3.3965	0.24204	89.141	21.801	13.529	32.149
	36	133	6	798	3.1968	0.04234	70.166	2.8258	33.46	12.218
	484	1541	6	9246	3.1771	0.02264	67.845	0.5048	47.979	2.3007
	5476	16725	6	100350	3.1771	0.02264	67.702	0.3618	55.943	10.265

Fig. 6.21: Results from the software analyses

By comparing the seperate elements individually the best representative can be chosen:

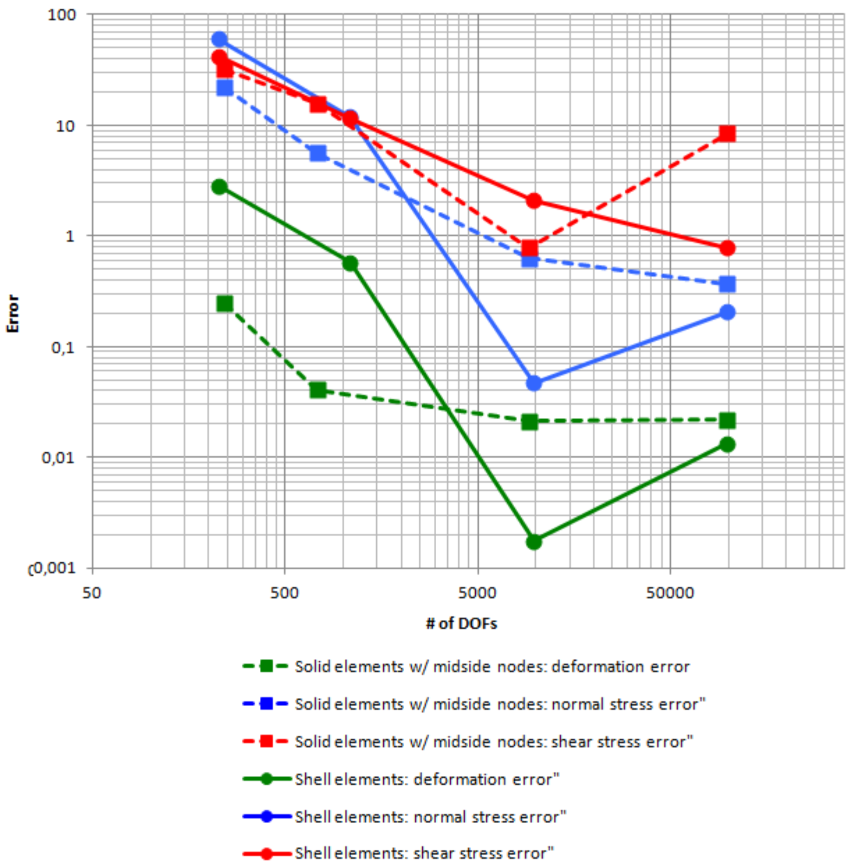

Fig. 6.22: Comparison of the solid elements

Although the plain 8 noded hex elements have an unexpected kink in the graph, it is safe to conclude that the 20 noded hex element has a better consistency and is therefore the best choice.

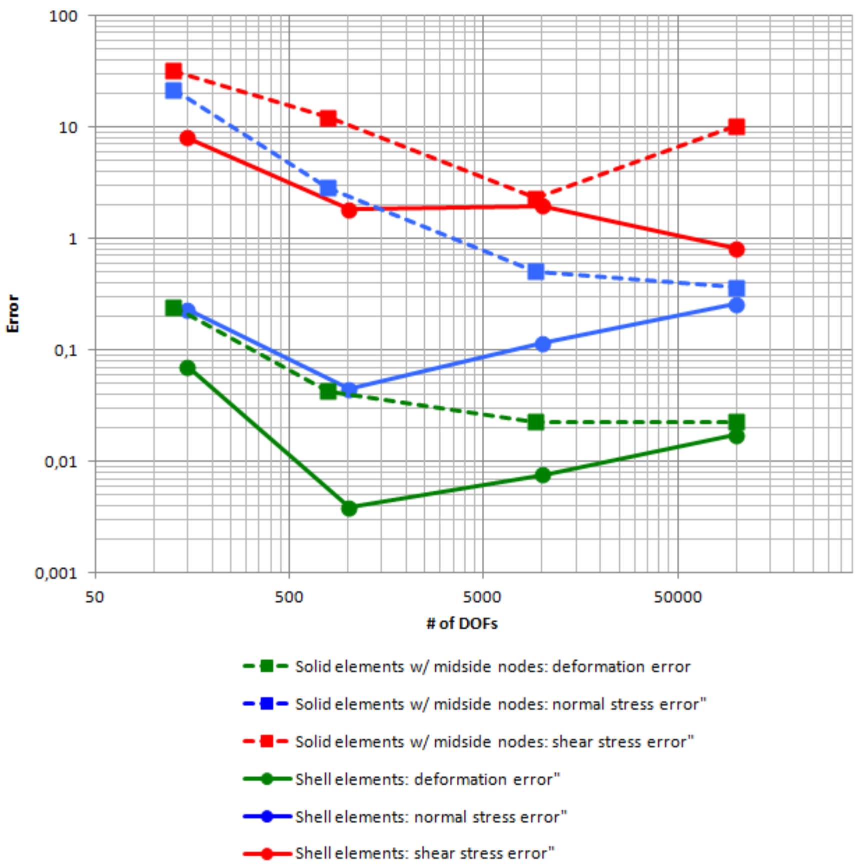

Fig. 6.23: Comparison of the shell elements

Here the R4 elements seem better, We compare the preferred ones from each element type:

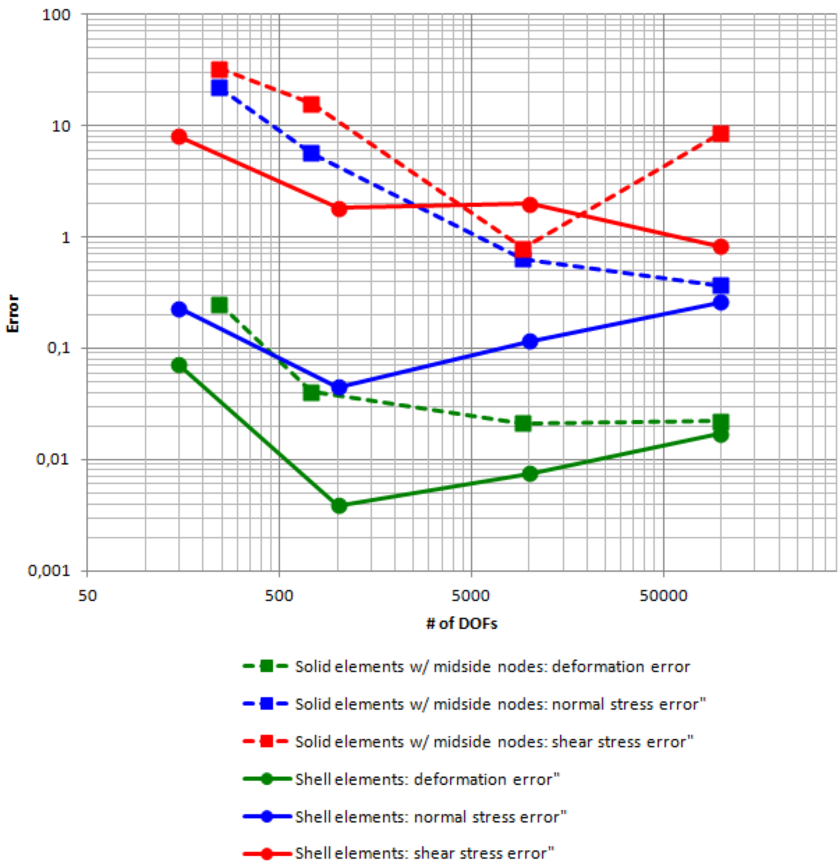

Fig. 6.24: Comparison of shell and solid elements

Even though a clearer correlation would be preferable, it can be concluded that shell elements are superior representation for thin plates when it comes to bending. The plated enclosure in the following analysis will therefore be represented by shell elements.

6.2 A simple blast load scenario

6.2.1 Assumptions

Since this scenario requires a non-linear analysis, the exact solution would be quite hard to acquire. A thorough analysis of the model, with a dense solid mesh for the framework and dense shell elements for the plates will therefore be run and used as the basis for comparison with the next cases.

The values we compare are:

- Equivalent Stress (Von-Mises)
- Total Deformation

6.2.2 The model

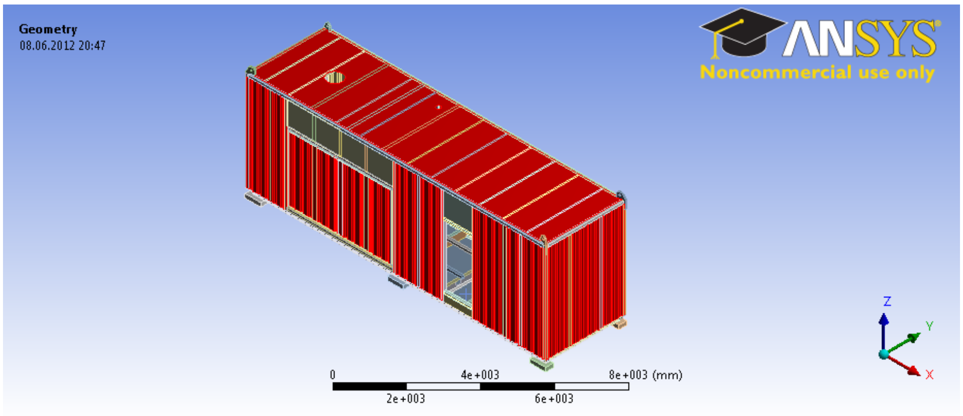

Fig. 6.25: The original model

The model of the complete module would take days to prepare and hours to analyse. Therefore this analysis will concentrate on a fraction equivalent to the simplest wall of the module. The spacing and dimension of the framework is identical, hence the plate profile is a little adjusted for the purpose of symmetry and consistency.

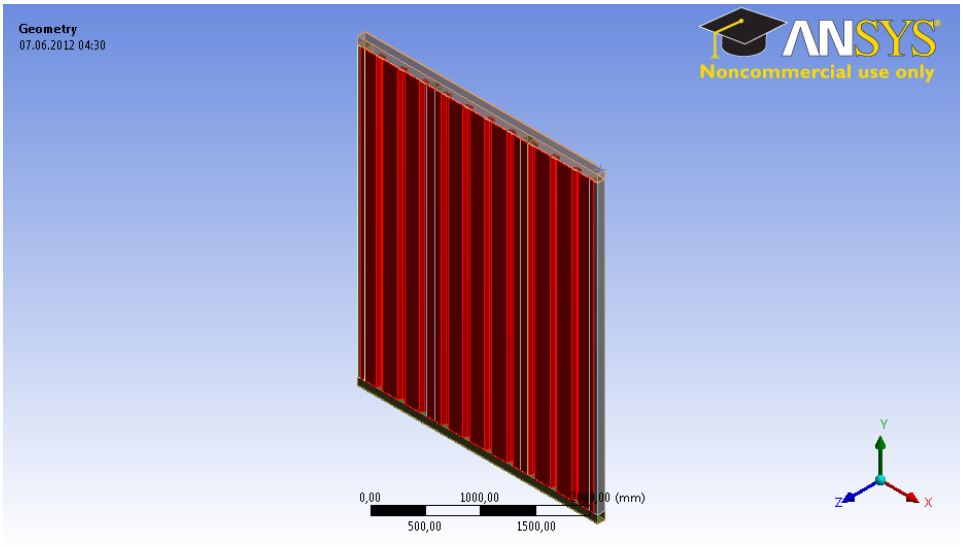

Fig. 6.26: The simplified model

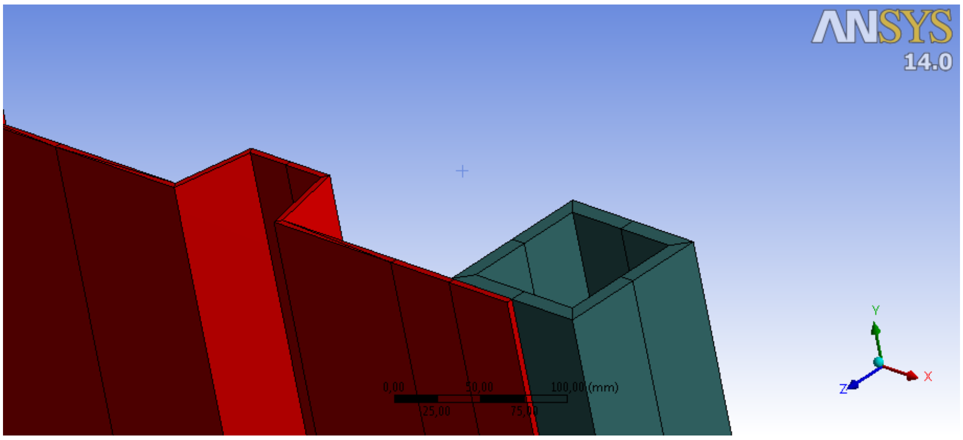

Fig. 6.27: A closer look at the plate profile

6.2.3 The thorough analysis

The framework is meshed as a solid model and the plate as a surface, like concluded in the previous section.

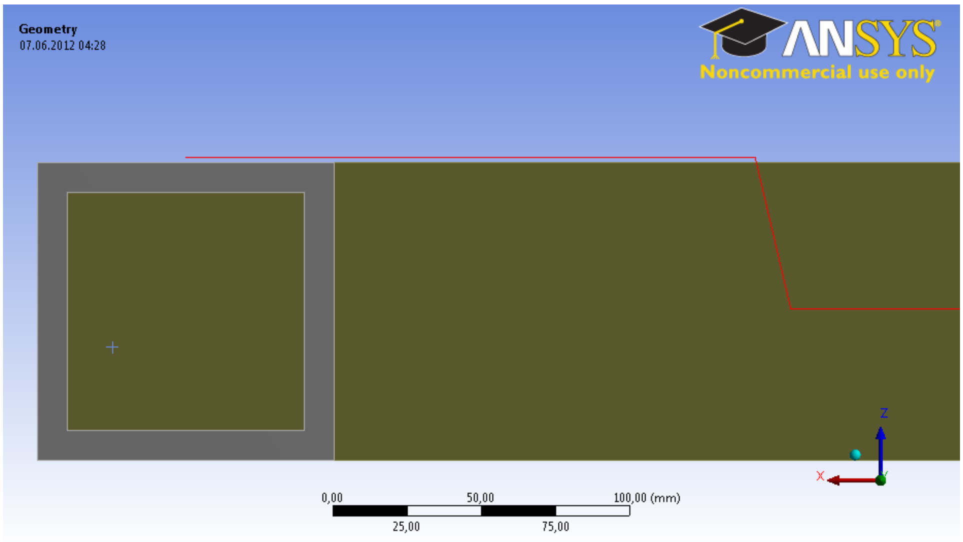

Fig. 6.28: Plate represented by surface leaves a gap equal to half the plate-thickness

The contact-conditions can still be set to bonded, regardless of the gap. It might need to be manually set if the tolerance for the auto detection is too low.

The set-up

- The plate is restrained to the framework through bonded connections
- The model has fixed supports in the the four outer beams
- A pressure of 0,03 bar is applied to the front over a short time period (see Fig 6.29)

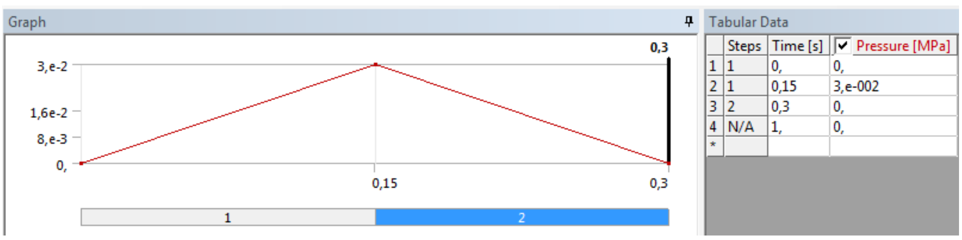

Fig. 6.29: The loading

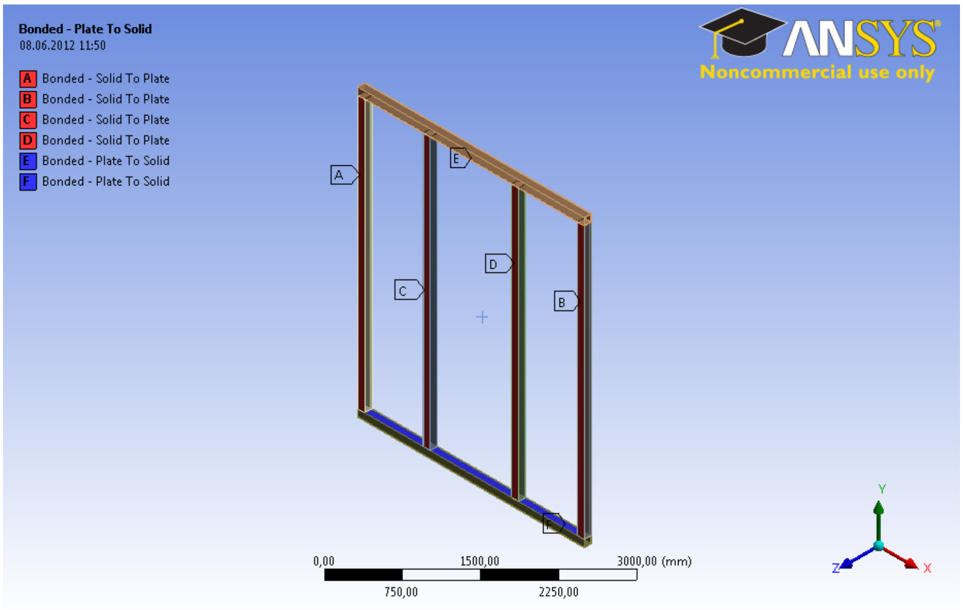

Fig. 6.30: Bonded connections between framework and plate

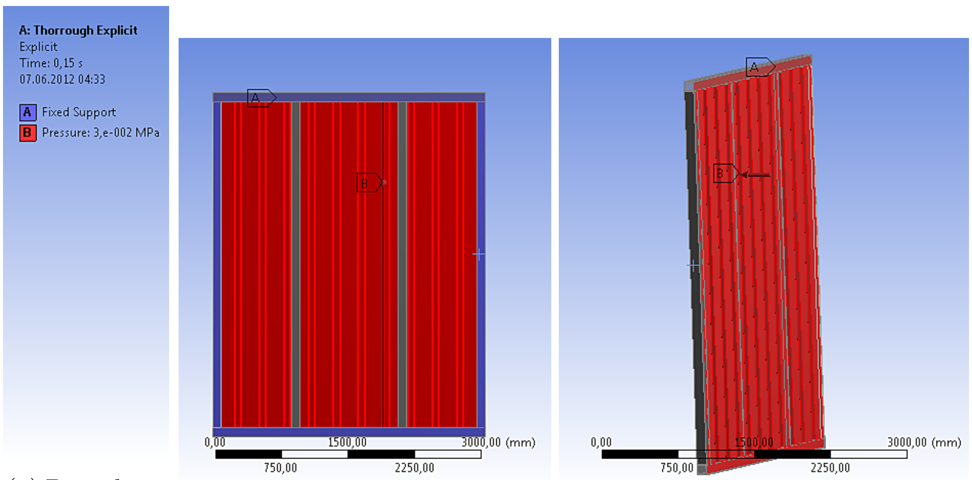

(a) Boundry Conditions

(b) Fixed Supports

(c) Pressure

Fig. 6.31: Boundry Conditions: Supports and loading

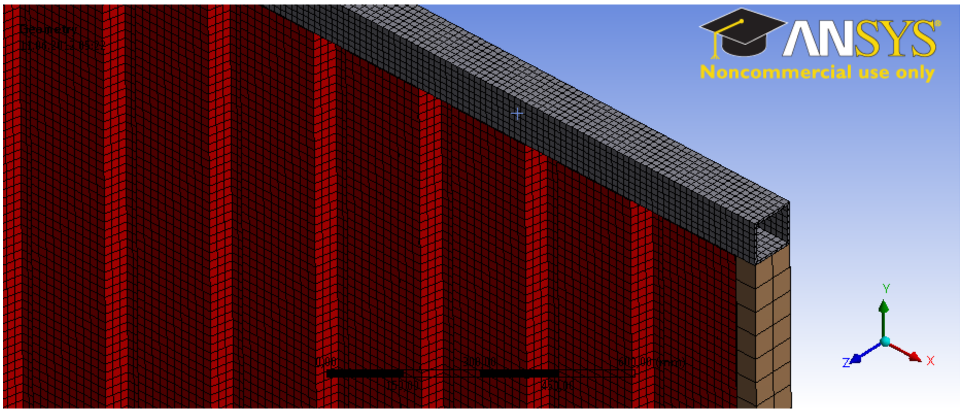

Fig. 6.32: The mesh

The Results

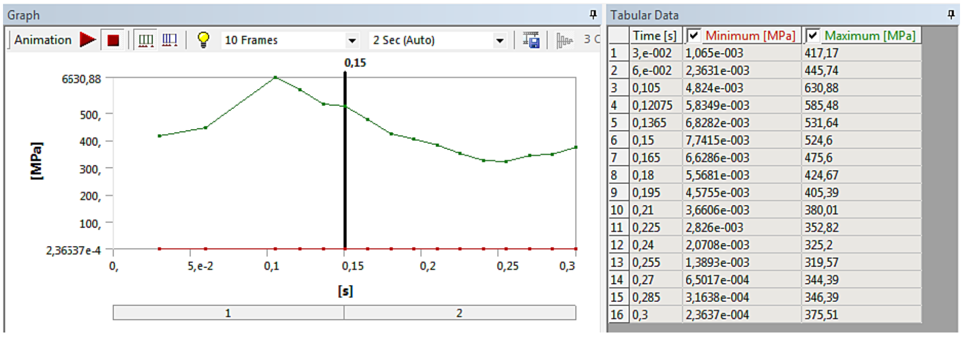

	Time [s]	Minimum [MPa]	Maximum [MPa]
1	3,e-002	1,065e-003	417,17
2	6,e-002	2,3631e-003	445,74
3	0,105	4,824e-003	630,88
4	0,12075	5,8349e-003	585,48
5	0,1365	6,8282e-003	531,64
6	0,15	7,7415e-003	524,6
7	0,165	6,6286e-003	475,6
8	0,18	5,5681e-003	424,67
9	0,195	4,5755e-003	405,39
10	0,21	3,6606e-003	380,01
11	0,225	2,826e-003	352,82
12	0,24	2,0708e-003	325,2
13	0,255	1,3893e-003	319,57
14	0,27	6,5017e-004	344,39
15	0,285	3,1638e-004	346,39
16	0,3	2,3637e-004	375,51

Fig. 6.33: Stress at time = 0.15sec

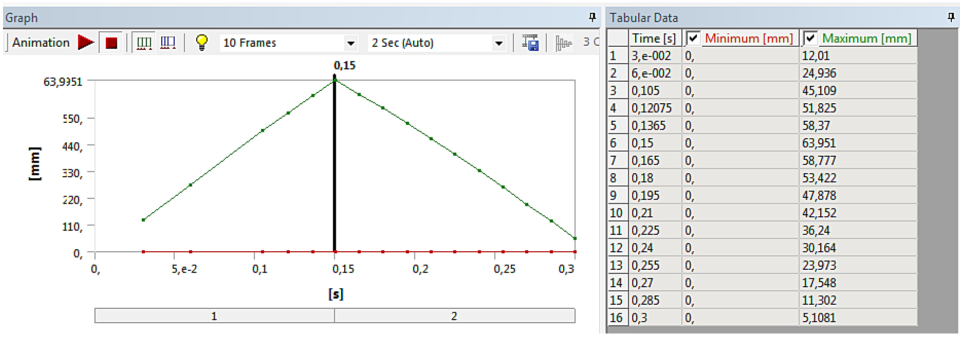

	Time [s]	Minimum [mm]	Maximum [mm]
1	3,e-002	0,	12,01
2	6,e-002	0,	24,936
3	0,105	0,	45,109
4	0,12075	0,	51,825
5	0,1365	0,	58,37
6	0,15	0,	63,951
7	0,165	0,	58,777
8	0,18	0,	53,422
9	0,195	0,	47,878
10	0,21	0,	42,152
11	0,225	0,	36,24
12	0,24	0,	30,164
13	0,255	0,	23,973
14	0,27	0,	17,548
15	0,285	0,	11,302
16	0,3	0,	5,1081

Fig. 6.34: Deformation at time = 0.15sec

Tab. 6.3: Results from thorough analysis

Max Equivalent stress [MPa]	524.6
Max Deformation [mm]	63.951

Because time increments may differ between the analyses (for a result to converge), the results at time=0.15sec will be the ones that are compared. To see if it is sufficient to run only the first load step (0-0.15 sec), another analysis with the same settings and reduced to 1 load-step:

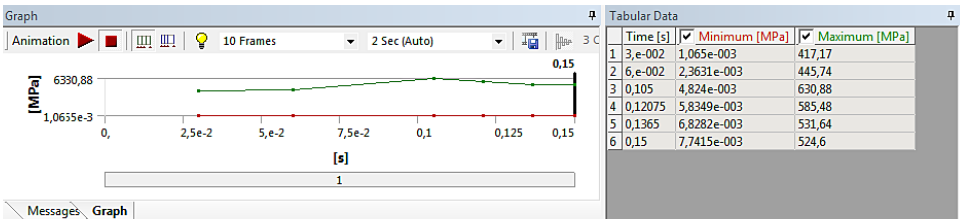

Fig. 6.35: Stress at time = 0.15sec

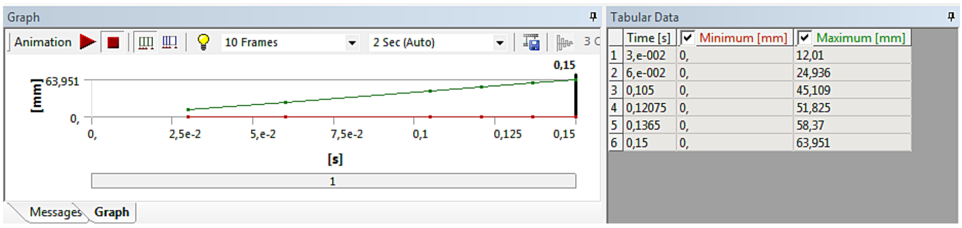

Fig. 6.36: Deformation at time = 0.15sec

Tab. 6.4: Results from shortened thorough analysis

Max Equivalent stress [MPa]	524.6
Max Deformation [mm]	63.951

Since the results are identical to the previous analysis, it is safe to conclude that computing only the first part of the blast load scenario will be sufficient to acquire the results at time 0.15sec.

The computation times can be compared to determine the time saved by running a shortened analysis:

$$\frac{8993.457s - 5263.131s}{8993.457s} = 0.415 = 41.5\%$$

The reason that it is not 50 % can be explained by the force convergence chart for the first analysis:

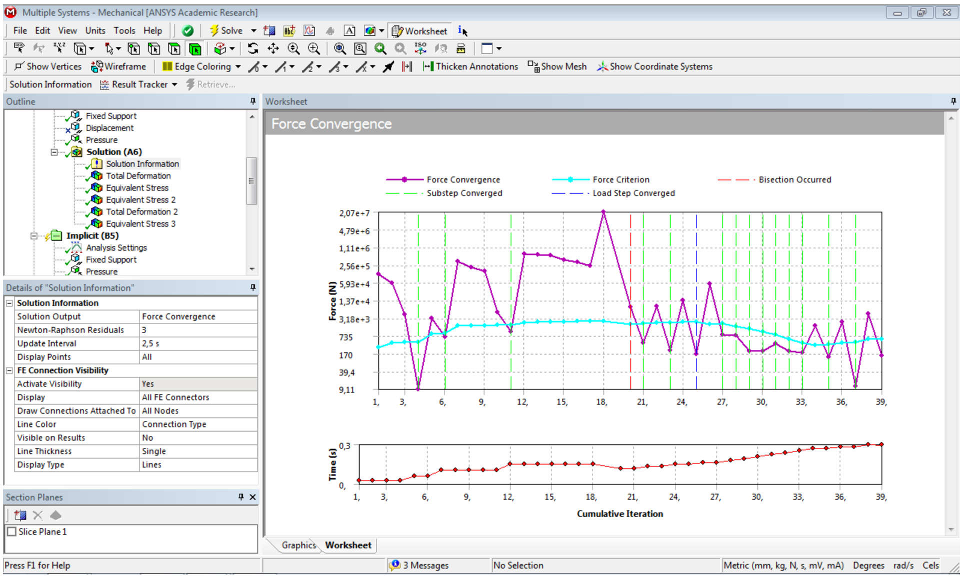

Fig. 6.37: Force Convergance chart

It is clear that force convergance is slower in the first load step.

6.2.4 Non-linear vs Linear

Reducing the material properties to linear behaviour and assuming no large deformations, makes it possible to run the analysis as a linear problem. The results are as follows:

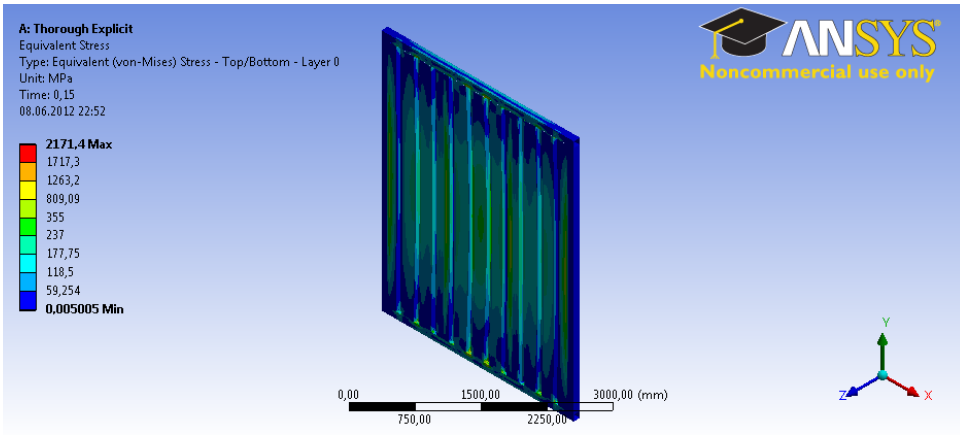

Fig. 6.38: Linear: Stress at time = 0.15sec

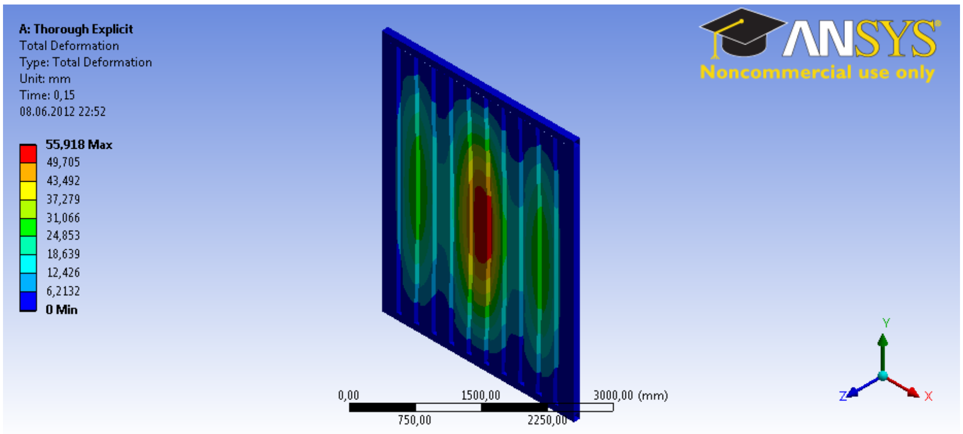

Fig. 6.39: Linear: Deformation at time = 0.15sec

Tab. 6.5: Results from the linear analysis

Max Equivalent stress [MPa]	2171.4
Max Deformation [mm]	55.918

Comparing this with the non-linear analysis shows that although the deformations are not too far off, the stresses are not even close to what they should be. This indicates that the linear material properties allows the stress to build up to infinity due to the assumption of a linear stress-strain relationship.

Because of insufficient memory to solve the non-linear analysis with an implicit solver, this linear analysis was run both explicit and implicit for comparison. The results were identical but the computation time for the explicit solver was 221.740 second versus 757.135 seconds for the implicit solver. The fact that the implicit solver takes 240 % longer, confirms that explicit is much faster for short time steps.

6.2.5 Simplified model, represented by shell elements

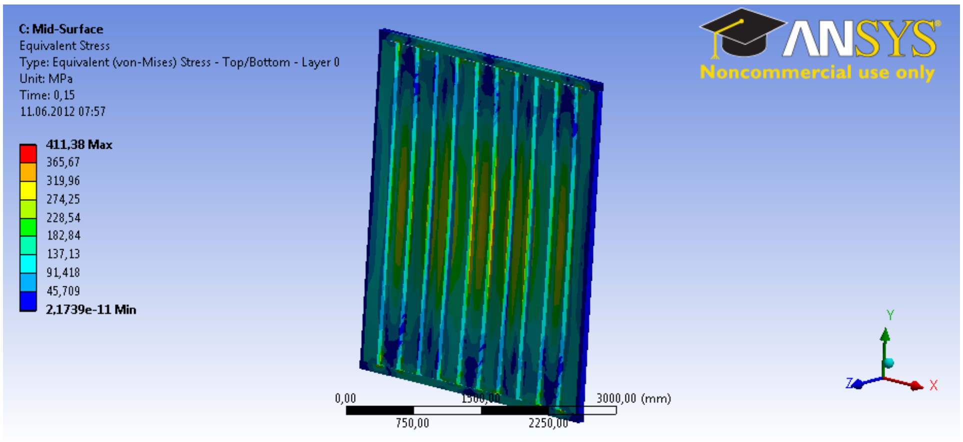

Fig. 6.40: mid-surface model: stress

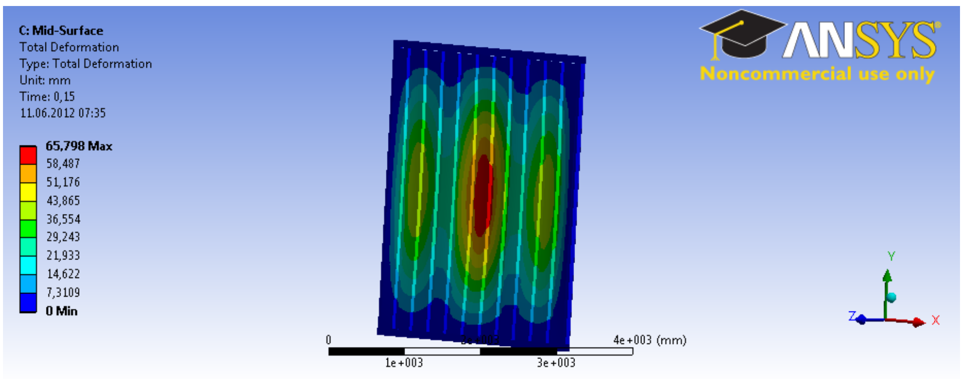

Fig. 6.41: mid-surface model: deformation

Tab. 6.6: Results from shell-model analysis

Max Equivalent stress [MPa]	411.38
Max Deformation [mm]	65.798

The deformation is pretty close to the thorough result, but the stress is a little off. By taking a closer look at the results from the thorough analysis and adjusting the colour grid, it can be observed that the stress exceeding 411,38MPa are very small and local:

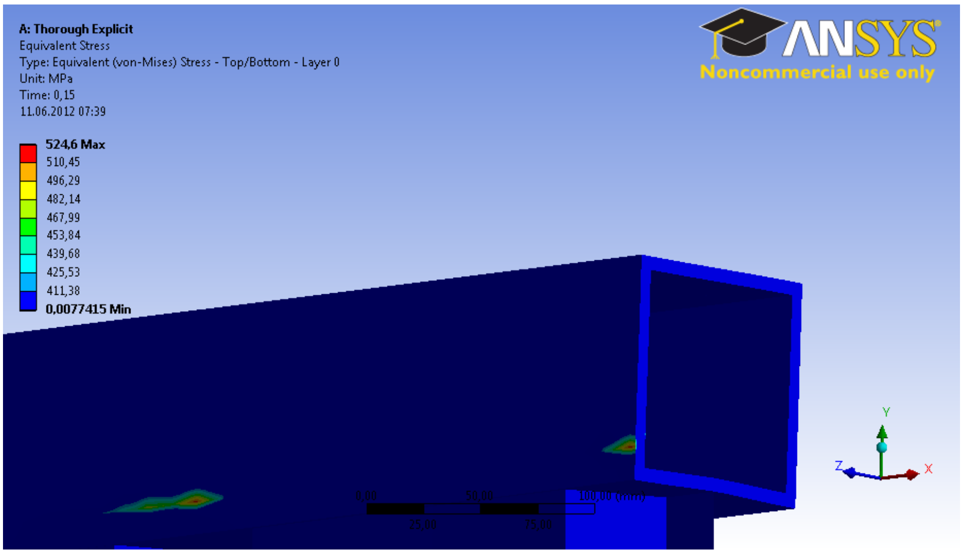

Fig. 6.42: Local stress in thorough analysis

Stress is typically associated with the second differentiation of deformation (recall eq. 6.6), thus the error of stress is expected to be larger than the error of deformation. Yet, the stress is a bit more off then expected. The local stress accumulation in the thorough analysis seems to be smaller than the element size in the shell-model mesh, and if the stress was averaged out with the surrounding nodes forming two identical meshes, the stress would probably fit better. The deviation could also be caused by poor contact conditions or poor mesh quality. Several different analyses have been run without any significant change. Nevertheless, as earlier mentioned, local stress concentrations are not the most important as long as structural integrity is intact. The overall stress distribution seems to match well, and it can be concluded that shell elements give a good representation of our model. It reduces the computation time dramatically, without significant loss of accuracy.

6.2.6 S355 vs AISI 316L

These results differ some from the thorough analysis, because of some changes made to the mesh. However, the same settings apply to both the analyses regarding material, and the comparison is therefore valid.

EN S355

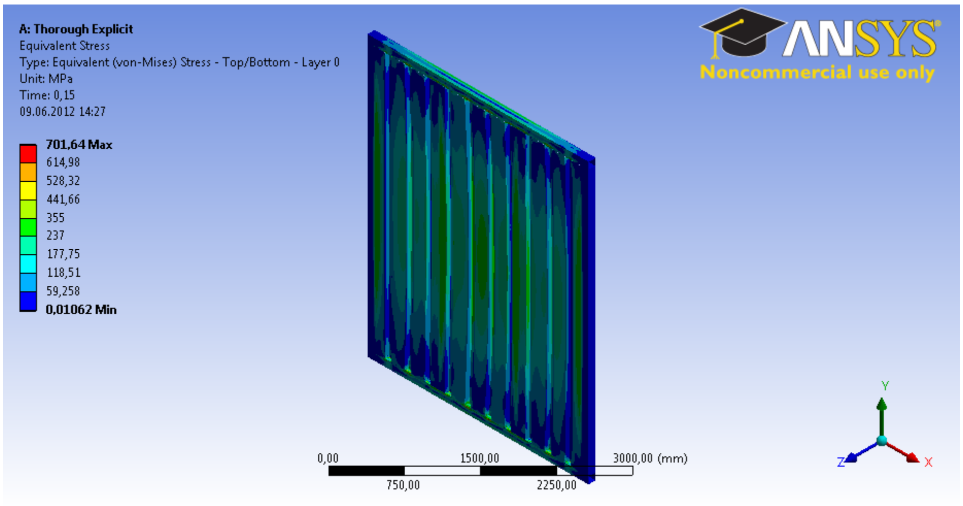

Fig. 6.43: EN S355 stress

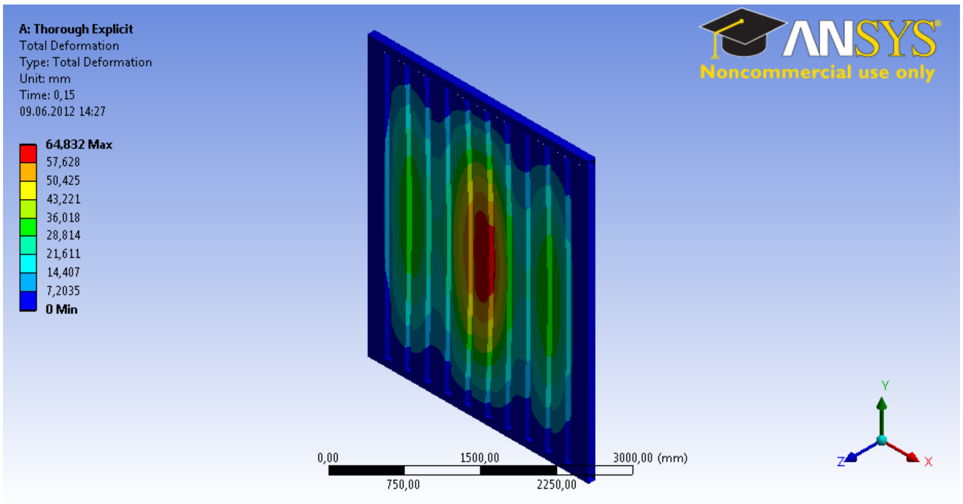

Fig. 6.44: EN S355 deformation

Tab. 6.7: Results from EN S355 analysis

Max Equivalent stress [MPa]	701.64
Max Deformation [mm]	64.832

AISI 316L

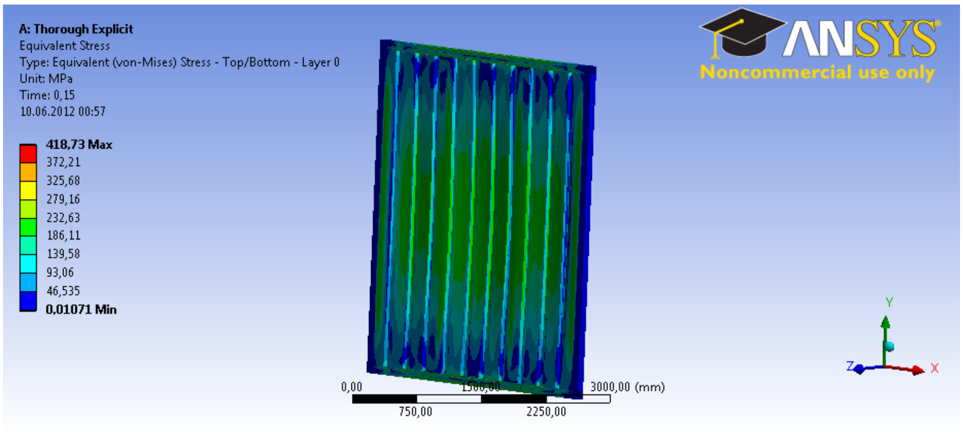

Fig. 6.45: AISI 316L stress

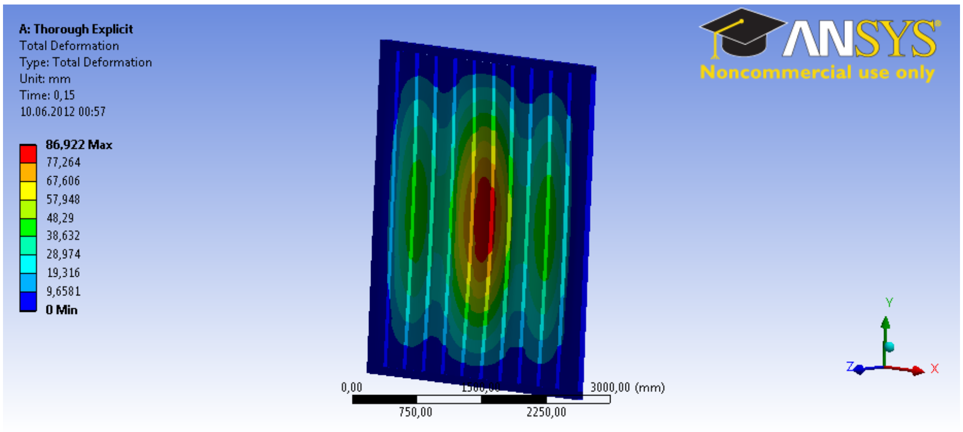

Fig. 6.46: AISI 316L deformation

Tab. 6.8: Results from ANSI 316L analysis

Max Equivalent stress [MPa]	418.73
Max Deformation [mm]	86.922

It is clear that the structural steel can withhold deformation better than the stainless steel. When it comes to stress however, the stainless steel has absorbed a significant amount and ensured that the material will not fail. This indicates that the plastic abilities for stainless steels play a significant role in blast load-scenarios.

7. SOFTWARE - COMMUNICATION

7.1 Problematic Scenarios

As mentioned earlier. The process of transferring the model from the design software to the analysis software and prepare it for analysis can be quite challenging. Especially when the model is as big and complex as a FWP module. There are tools created for these purposes, but they are not designed to give you a better overview of the model. The biggest problem is maybe keeping track of what has been done and what still needs to be done to simplify the model regarding unnecessary features and transforming solids into shell representation.

7.2 Suggestions to solutions

Some helpfull tools are:

- The "extract surface" feature in ANSYS Design Modeller
- A software called Space Claim

7.2.1 The "extract surface" feature

This feature is helpful for extending surfaces to intersect with another. Since the module will consist of hundreds of gaps that need to be closed, selecting each surface to extrude individually is obviously very tedious work. However, with the the newest version of Ansys (14), there is an automatic selection" option, where it is possible to choose a threshold for the gaps that should be closed. For instance, choosing "gap = 5" will select all surfaces that can be extended 5mm or less to close a gap.

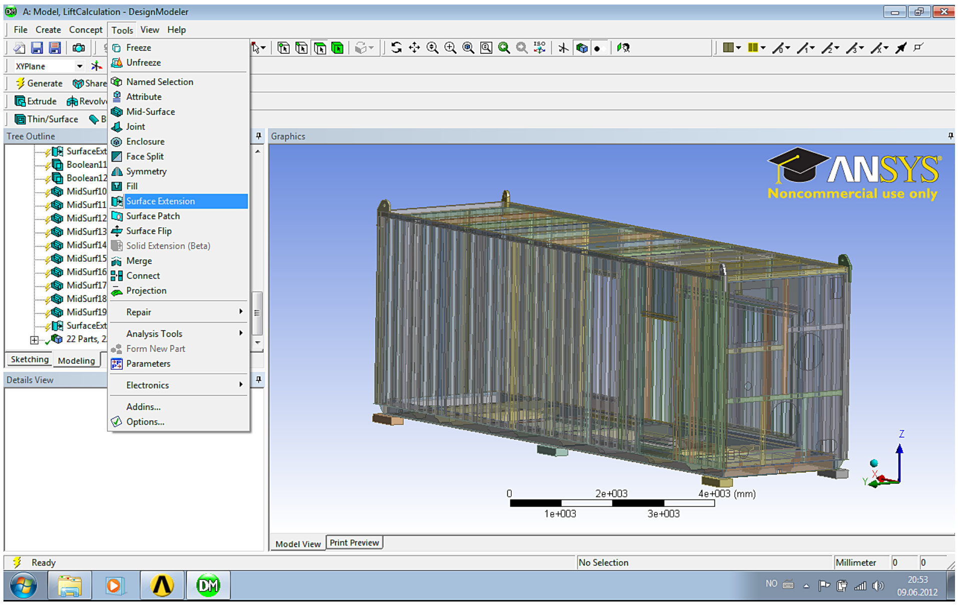

Fig. 7.1: Surface Extraction

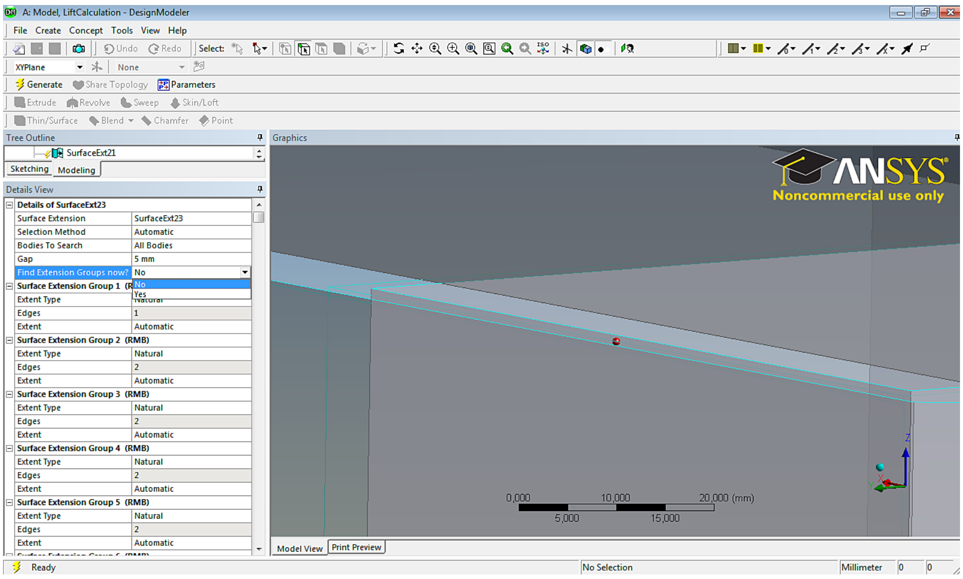

Fig. 7.2: Surface Extraction

7.2.2 *Ansys SpaceClaim*

SpaceClaim is an untraditional *CAD*-software, that is not utilizing the traditional *model-tree*. The advantage here is that modifying features will less likely conflict with features that are fixed in a model tree. SpaceClaim is very interactive and easy to use, and it has a designated modify/prepare mode where the purpose is to simplify and prepare models for analyses. It has features like "Remove Radius/Chamfer" amongst others.

After attending a seminar at EDR's [1] office in Oslo, they were happy to offer a try out of their new integrated version; *Ansys SpaceClaim*. SpaceClaim has been an individual software for some time, but has recently started a collaboration with the creators of ANSYS.

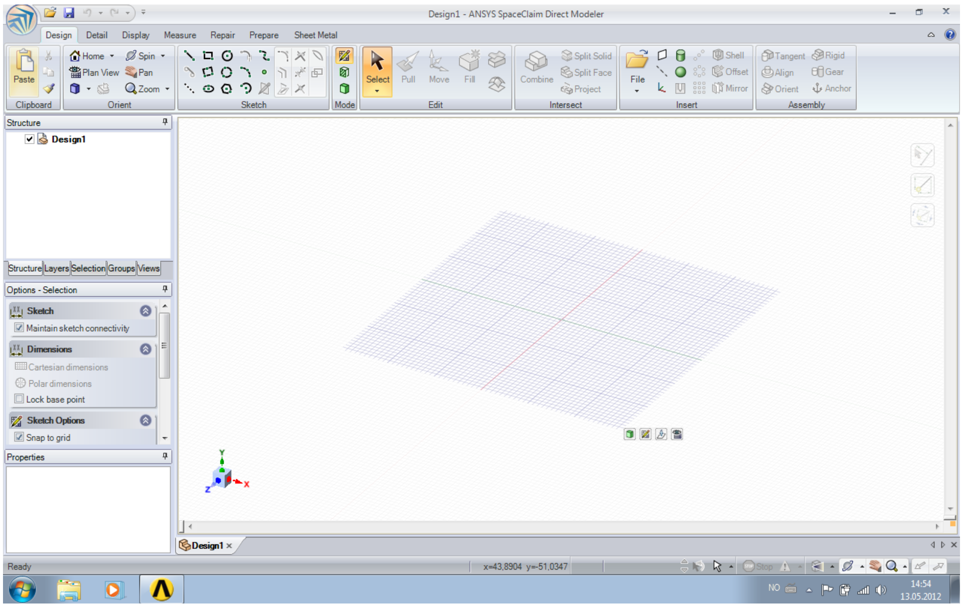

Fig. 7.3: Space Claim Interface

[1] The distributor of ANSYS

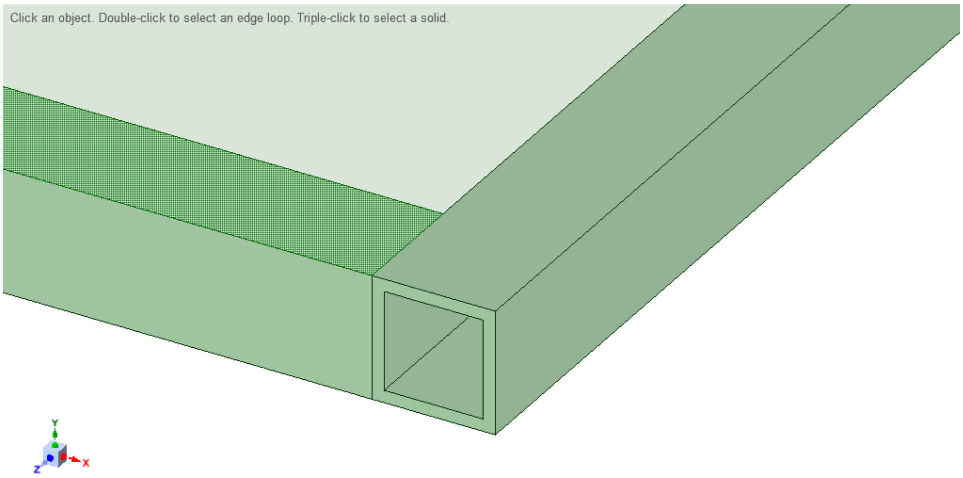

Fig. 7.4: Building a frame

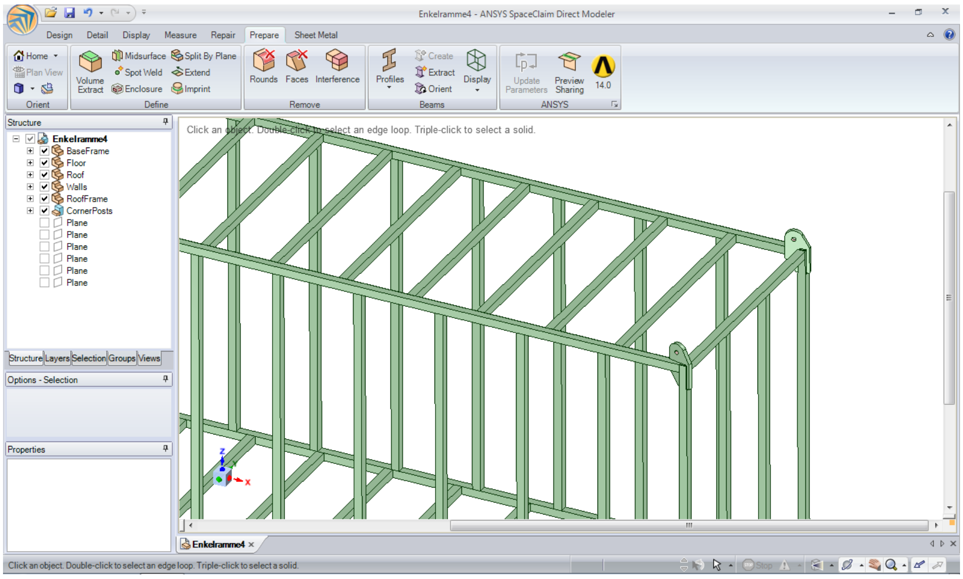

Fig. 7.5: The "prepare-mode"

7.3 A simplified baseframe

To get to know the *SpaceClaim* software better it was natural to create a new scenario and build the model in SpaceClaim. Like in the previous section, the model is significantly simplified. But it serves the purpose of presenting the analysis-preparation process. For the purpose of convenience all the beams are 100mm x 100mm with a wall thickness of 10mm.

7.3.1 Assumptions

In a lift operation we usually use a sling system which makes sure that the crane is stable and above the module's *COG* [2].

Placing the lift-point above the COG of the model will ensure stability for the the static analysis

7.3.2 The model

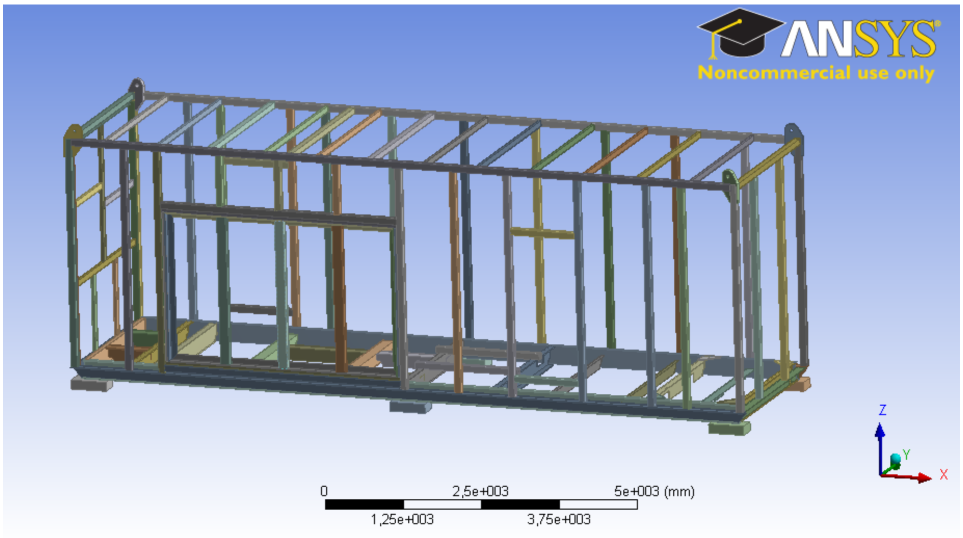

Fig. 7.6: The original model

[2] Centre of Gravity

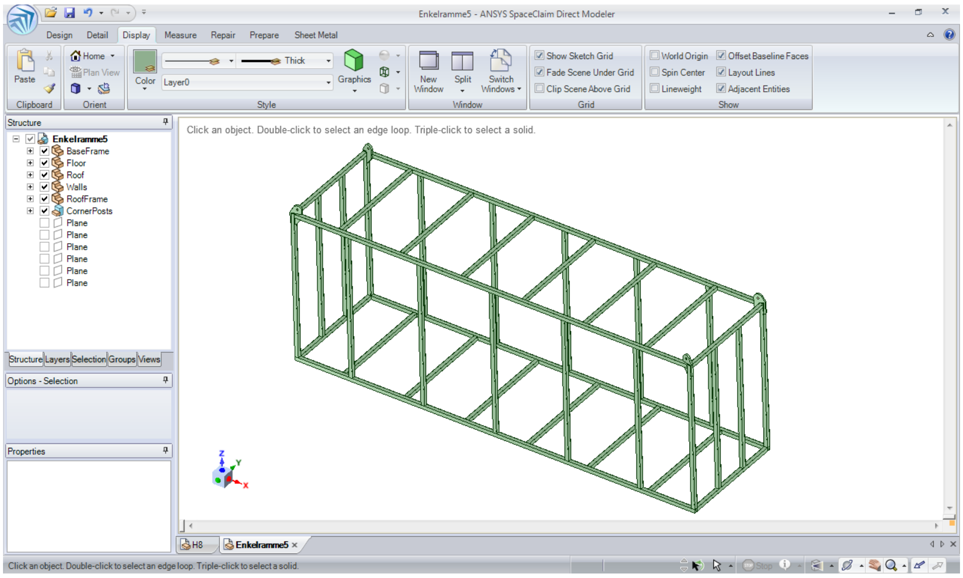

Fig. 7.7: The simplified model

7.3.3 *Use of ANSYS to transform solid model into mid-planes*

The process of transforming a solid model into a "mid-surface" model is tedious work. But since the simplified model is symmetric and consistent, the auto-select feature can make the process fairly comfortable. All the beams have 10mm as the thickness in their cross-section. So by specifying this in the auto-select feature. All the beams will be transformed in one singel operation:

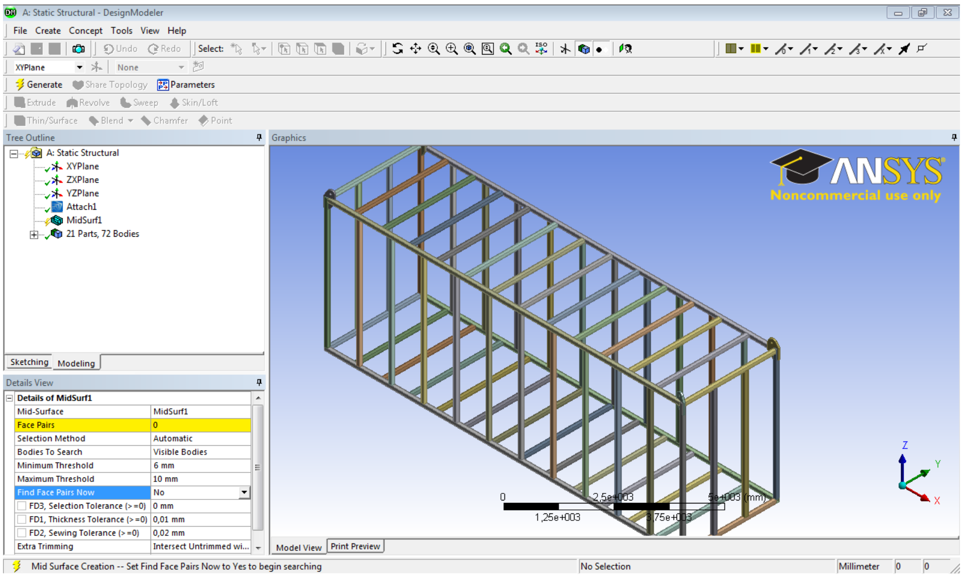

Fig. 7.8: Use "Auto select" to select the beams

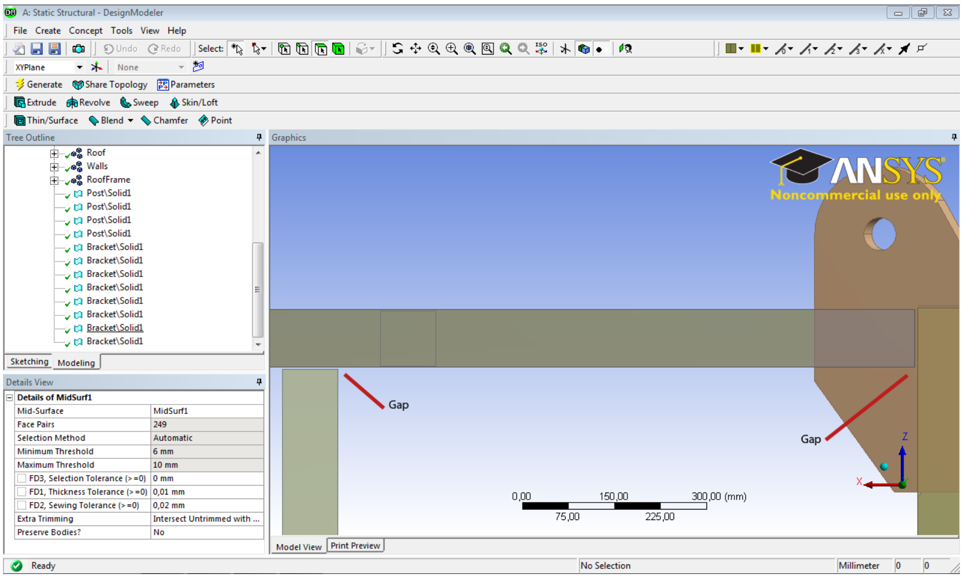

Fig. 7.9: Found and transformed 255 facepairs

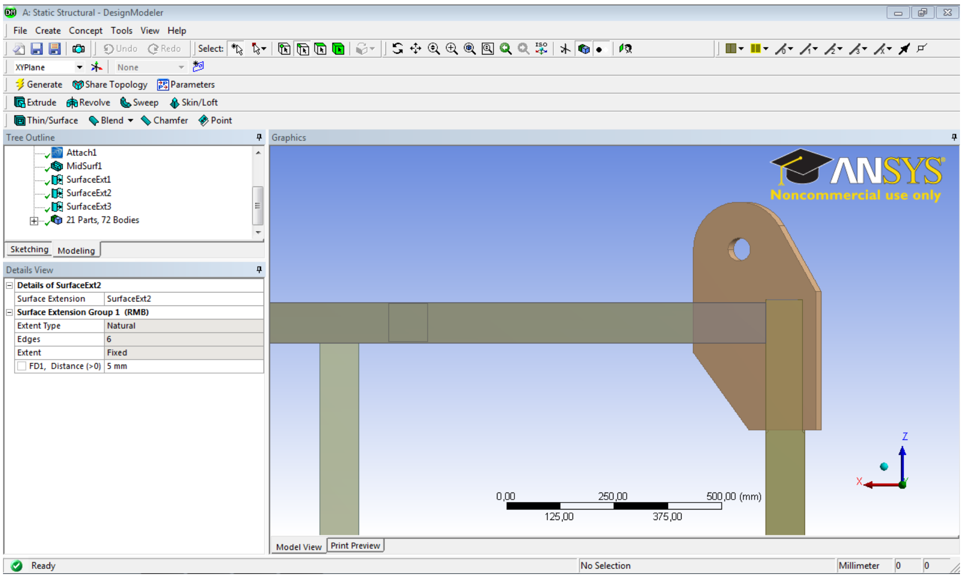

Fig. 7.10: The gaps are easily closed with the surface extension feature, using "gap"=5mm

The model is now represented by surfaces, except for the pad-eyes that are still solids (they are thicker than the threshold/tolerance chosen in the auto-find feature). This concludes the preparation of the model and after determining the lift point, the analysis can be set up and run. This will not be covered in the thesis, but could be interesting to look at in further research.

7.3.4 Lift Point

The cables that are used to lift the original model are 12m long and has a diameter of 48mm.

From the software we can determine the centre-point of the holes in the pad-eyes, they are as follows

Tab. 7.1: Padeye centres

PadEye #	x [mm]	y [mm]	z [mm]
1	150.38	71.897	4365
2	150.38	3018.1	4365
3	11330	71.897	4365
4	11330	3018.1	4365

The lift wire length is 12m, and through simple trigonometry (presented in B) the origin for the lift point can be determined to be:

Tab. 7.2: Lift Point

	x [mm]	y [mm]	z [mm]
Lift Point	5740	1545	14881

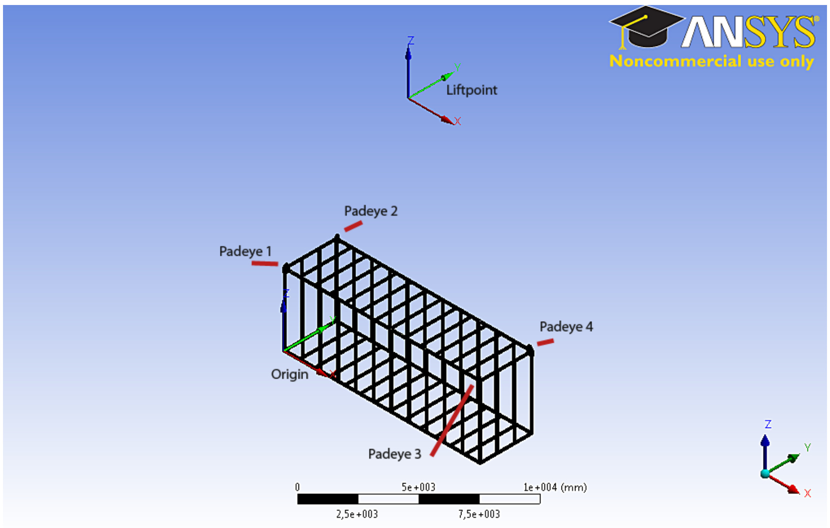

Fig. 7.11: The coordinate system

8. CONCLUSION

The analysis process is the major bottleneck in the production of FWP systems. Because of high requirements to safety there is no room for shortcuts, and Framo has to make sure their products meet all the standards. This thesis presents some of the different ideas to decrease the delay caused by the analysis process.

A preliminary analysis is carried out, comparing exact values with results from simple software analyses. The basis is a simple plate problem that satisfies Navier's plate equation. Through this equation exact values are presented and used to compare different elements and meshes when it comes to error. The preliminary analysis concludes that shell elements are the best representation for plated structures subject to pressure.

Next a blast-load analysis is carried out. The model is based on the result from the preliminary analysis, with shell elements representing the plate and solid elements representing the framework. This first blast load analysis is carried out with a dense mesh to assure as exact results as possible. These results are the basis for comparison with different settings. In a blast load scenario, the maximum experienced deformation and equivalent stress is within the first load step. Through comparison it is proven that running only the first load step in an analysis will not jeopardise the results. This observation will reduce the computation time significantly.

An implicit solver gave the same results as the explicit, but in the particular case where short time steps are necessary, it requires significantly more memory and computation time. Using explicit solver when it is appropriate, such as is the blast load case, will also reduce the computation time significantly.

In blast loading, the material's plastic properties plays a big role. This is proven by studying a linear material model. A non-linear analysis is required to ensure reliable results. Stainless steel is superior to construction steel when it comes to blast loading. This is because of it's plastic properties.

Representing the whole model with shell elements is a good approximation to reduce computation time, and yet preserving accurate results if the stress distribution is smooth.

Finally some features in Ansys, that will reduce the time consuming work of preparing a model for analysis, are presented.

8.1 Further Work

Because the computations themselves are tedious and time consuming, there was not enough time to explore all the choices available. Therefore there is still room for more comparisons for the blast load-model.

It would also be interesting to find a clearer correlation between number of DOF's and error, in the preliminary analysis. This will require more points on the graph.

As mentioned in the chapter 4, a study and derivation of material indices would be interesting and might also be rewarding for the company, in terms of finding optimal materials for different requirements.

It would be interesting to run a lift analysis on the simplified model of the baseframe presented in section 7.3.

9. LITERATURE

[1] Framo FWP-module static report number 1691-175-4: Pazflor FPSO FWP

[2] "Concepts and Applications of Finite Element Analysis" by Robert D. Cook, David S. Malkus, Michael E. Plesha and Robert J. Witt. ISBN:978-0-471-35605-9

[3] "Steel Structures: Design using FEM" by Rolf Kindmann and Matthias Kraus. ISBN:978-3-433-02978-7

[4] Lecture notes from TKT4192: Finite Element Methods in Strength Analysis by Kjell H. Holthe

[5] Lecture notes from TKT4197: Nonlinear Finite Element Analysis By Kjell Magne Mathisen

[6] Lecture notes from TKT4124: Mechanics 3 By Aase Gavina Roberg Reyes

[7] "Advanced mechanics of materials, 2nd Edition" by Robert D. Cook and Warren C. Young. ISBN:0-13-396961-4

[8] The "Meshing" user manual for Ansys 14

[9] Offshore Standard DNV-OS-C101: Design of offshore steel structures, General (LRFD Method)

[10] "Ship-Shaped Offshore Installations: Design, Building and Operation" by Jeom Kee Paik and Anil Kumar Thayamballi. ISBN: 978-0-521-85921-9

[11] http://www.matweb.com

APPENDIX

A. MATLAB SCRIPT

```
% Choosing parameters

error_limit=eps;

N=101; % # of nodes = n^2

q0=0.015; %N/mm^2
a=500; %mm
b=500; %mm
h=2; %mm
z=2; %mm
E=206000; %N/mm^2
v=0.3;
D=2*E*h^3/(3*(1-v^2)); % N*mm

x=linspace(0,a,N);
y=linspace(0,b,N);


m=0;
n=2;

%Creating empty matrices
w=zeros(N,N);
sigma_x=zeros(N,N);
sigma_y=zeros(N,N);
sigma_xy=zeros(N,N);


while n>1
    n=0;
    m=m+1;
```

```
    factor=1;
    while factor>=error_limit
        n=n+1;
        factor=(16*q0)/(((2*m-1)*(2*n-1)*D*(pi^6)*((2*m-1)^2/a^2...
         +(2*n-1)^2/b^2)^2));
        matrix=sin((2*m-1)*pi*x'/a)*sin((2*n-1)*pi*y/b);
        w=w+factor*matrix;

        sigma_x=sigma_x-((z*E)/(1-v^2))*factor*(((2*m-1)*pi/a)^2...
         *(-sin((2*m-1)*pi*x'/a))*(sin((2*n-1)*pi*y/b))+(v*(sin((2*m-1)...
         *pi*x'/a)*((2*n-1)*pi/b)^2*(-sin((2*n-1)*pi*y/b)))));

        sigma_y=sigma_y-((z*E)/(1-v^2))*factor*((sin((2*m-1)*pi*x'/a)...
         *((2*n-1)*pi/b)^2*(-sin((2*n-1)*pi*y/b)))+(v*((2*m-1)*pi/a)^2...
         *(-sin((2*m-1)*pi*x'/a))*(sin((2*n-1)*pi*y/b))));

        sigma_xy=sigma_xy-((z*E)/(1-v^2))*(1-v)*factor...
         *(((2*m-1)*pi/a)*cos((2*m-1)*pi*x'/a))...
         *(((2*n-1)*pi/b)*cos((2*n-1)*pi*y/b));
    end
end


figure(1)
surf(x,y,w)
xlabel('x [mm]')
ylabel('y [mm]')
zlabel('w [mm]')
colorbar
figure(2)
surf(x,y,sigma_x)
view([0 90])
xlabel('x [mm]')
ylabel('y [mm]')
title('\sigma_x [MPa]')
colorbar
figure(3)
surf(x,y,sigma_y)
view([0 90])
xlabel('x [mm]')
ylabel('y [mm]')
title('\sigma_y [MPa]')
colorbar
figure(4)
```

```
surf(x,y,sigma_xy)
view([0 90])
xlabel('x [mm]')
ylabel('y [mm]')
title('\tau_{xy} [MPa]')
colorbar

%Displaying maximum values:

w_max=max(max(w))
sigmax_max=max(max(sigma_x))
sigmay_max=max(max(sigma_y))
tau_max=max(max(sigma_xy))
```

B. CALCULATING LIFT POINT

Tab. B.1: Padeye centres

PadEye #	x [mm]	y [mm]	z [mm]
1	150.38	71.897	4365
2	150.38	3018.1	4365
3	11330	71.897	4365
4	11330	3018.1	4365

$$L_x = \frac{11330 - 150.38}{2} = 5589.81$$

$$L_y = \frac{3018.1 - 71.897}{2} = 1473.1015$$

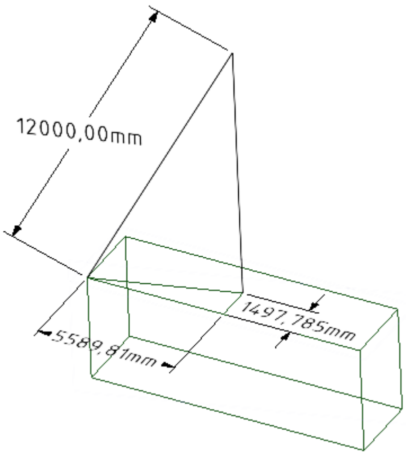

Fig. B.1: Lift Point Calculation

$$L_z = \sqrt{12000^2 - 5589.81^2 - 1473.1015^2} = 10515.89$$

$$x = L_x + 150.38mm = 5740.19mm$$

$$y = L_y + 71.897mm = 1545mm$$

$$z = L_z + 4365mm = 14880.89mm$$

Tab. B.2: Lift Point

	x [mm]	y [mm]	z [mm]
Lift Point	5740	1545	14881